Available online at www.sciencedirect.com
SCIENCE DIRECT
Marine Micropaleontology 65 (2007) 137–162
MARINE MICROPALEONTOLOGY
www.elsevier.com/locate/marmicro

Radiolaria as a reflection of environmental conditions in the eastern and southern sectors of the Indian Ocean: A new statistical approach

John Rogers *, Patrick De Deckker

Department of Earth and Marine Sciences, The Australian National University, Canberra, ACT 0200, Australia

Received 3 November 2006; received in revised form 2 July 2007; accepted 2 July 2007

Abstract

Cluster analysis and species abundance plots of radiolarian abundance counts from core tops from the eastern Indian Ocean between 12° S and 31° S, and the southern Indian Ocean between 31° S and 62.5° S, demonstrate the existence of environmentally-related provinces supporting distinct taxa assemblages. These provinces are closely associated with currents in the eastern sector of the Indian Ocean and with fronts in the southern sector.

The radiolarian assemblages correlate strongly with salinity-normalised total alkalinity (NTA) at the sea-surface, with temperature, salinity, and density from the sea-surface to 300 m, and with dissolved oxygen and nitrate and phosphate concentrations from the sea-surface to 100 m. Palaeo-reconstructions of these parameters at the sea-surface have been made for six Last Glacial Maximum (LGM) samples from five eastern Indian Ocean cores. The LGM sea-surface temperature estimates are comparable with those based on planktonic foraminiferal counts of the same samples obtained by other researchers. The reconstructions show that, since the LGM, density increased markedly along the Western Australian coast south of 20° S but changed little further from the Western Australian coast. By contrast, phosphate concentrations were marginally lower than modern values along the Western Australian coast south of 20° S but more than twice modern values in the other LGM samples.

The utility of various regression and calibration techniques is discussed. It is concluded that, probably due to the effects of differences in radiolarian habitat, ocean currents, and/or environmental gradients, only one method, weighted averaging — partial least squares, is reliable in a study area of this size and complexity. If other methods are to be used, the study area must be partitioned into at least two separate regions with the major split between the eastern and southern sectors of the Indian Ocean.

Keywords: Radiolaria; taxa groupings; palaeo-reconstruction; WADE index; URI; alkalinity; SST; salinity; density; dissolved oxygen; nitrate; phosphate; WA-PLS; Leeuwin Current; LGM

1. Introduction

This paper describes the results of the analysis of radiolarian abundances from core tops collected in two rectangular areas of the Indian Ocean: the eastern sector which lies between 12° S and 31° S and between 107.7° E and 127.8° E and the southern sector between 31° S and 62.5° S and between 49.8° E and 110.6° E. Both the distribution of the radiolarian taxa and the relationship of their assemblages with oceanic parameters are discussed.

This study's objective in analysing radiolarian abundance data from relatively poorly-investigated eastern sector of the Indian Ocean and the better-studied southern sector is, firstly, to discover any distinguishable radiolarian

* Corresponding author. Fax: +61 2 6125 5544.
E-mail address: john.rogers@ems.anu.edu.au (J. Rogers).

0377-8398/$ - see front matter © 2007 Elsevier B.V. All rights reserved.
doi:10.1016/j.marmicro.2007.07.001

assemblages and, then, to decide which are the major environmental variables determining the composition of these assemblages (the *explanatory variables*). Finally, the study aims to reconstruct palaeoenvironmental conditions from fossil core samples.

The study sought to treat the two sectors of the Indian Ocean as a single unit with the expectation that the southern sector results might provide a basis for comparison for eastern sector core samples for glacial periods. An extensive survey of the available statistical regression and calibration methodologies has been necessary to find a valid technique to achieve this end. Only one method, weighted averaging-partial least squares (WA-PLS), meets the requirement.

Most previous investigations of Radiolaria in surface sediments from the eastern and southern Indian Oceans were conducted in the period 1965–1990. Petrushevskaya (1967) examined an area between approximately 10° N and 70° S and 20° E and 180° E, and found Antarctic, bipolar (Arctic- and Antarctic-dwelling), warm water, cool water, and cosmopolitan species. She identified some associations between species, but did not describe larger assemblages. Howard and Prell (1984) sought to explain differences in magnitude and timing between estimates of Last Glacial Maximum (LGM) SSTs based on Radiolaria from cores in the southern Indian Ocean and those based on foraminifera. Dow (1978) reconstructed palaeotemperatures in 36 trigger-core tops taken from an area between approximately 40° S and 65° S and 80° E and 120° E using Q-mode factor analysis (QMFA).

Johnson and Nigrini (1982) analysed Radiolaria in the eastern Indian Ocean between 10° N and 52° S and 81° E and 115° E as a complement to their earlier study of the western Indian Ocean (Johnson and Nigrini, 1980). They identified six recurrent groups of Radiolaria and nine radiolarian assemblages. They related the assemblages to various oceanographic conditions including currents and physico-chemical parameters. Morley (1989) studied the southern Indian Ocean between 31.7° S and 59.0° S and between 27.3° E and 130.0° E and identified four geographically distinct radiolarian assemblages and generated a transfer function for summer and winter SSTs. Granlund (1986) investigated the morphology of *Antarctissa* in the southern sector and concluded that the shape of the genus is influenced by temperature and salinity.

The environmental data used in our study is derived from the US Government National Office of Oceanic and Atmospheric Administration's (NOAA) World Ocean Atlas 2001 (WOA01, 2001). The Atlas provides objectively analysed data for nine major ocean parameters on annual, seasonal, and monthly time scales. These high quality data postdate those available to most previous researchers.

Many of the eastern Indian Ocean samples used in the present study have previously been analysed for clays (Gingele et al., 2001), pollen (van der Kaars and De Deckker, 2003), calcareous nannofossils (Takahashi and Okada, 2000), planktonic foraminifera (Martínez et al., 1998), benthic foraminifera (Murgese and De Deckker, 2005), and dinoflagellates (Young, 2006). The southern sector samples have been studied in relation to biogenic silica distribution and accumulation (Pichon et al., 1992; Bareille et al., 1998), detrital flux origin (Bareille et al., 1994), SST in comparison with the Vostok core findings (Waelbroeck et al., 1995), hydrographic changes (Labeyrie et al., 1996), the sediment redistribution by bottom currents (Dezileau et al., 2000), the barium distribution in surface sediments (Fagel et al., 2002), and authigenic uranium enrichment in glacial sediments (Dezileau et al., 2002).

2. Oceanographic setting

2.1. The southern Indian Ocean

The southern Indian Ocean has two major features. Firstly, it has, in essence, only one major current, the Antarctic Circumpolar Current (ACC), whose eastward flow is virtually unhindered. Because the permanent thermocline reaches the surface at the Subtropical Convergence (around 30° S), the ACC is equivalent barotropic, i.e. it is not restricted to the first few hundred metres of water depth but extends deeply enough to be affected significantly by the topography of the ocean floor (Tomczak and Godfrey, 1994). Secondly, the ocean is divided by a series of fronts which run approximately latitudinally (Fig. 1) (Tomczak and Godfrey, 1994; Belkin and Gordon, 1996). Both the positions of the fronts and the rates at which their associated waters sink are known to vary both seasonally and interannually, but the amplitude of the changes is not well established. The Polar and Subantarctic Fronts are more stable than the Subtropical Fronts which may change markedly between seasons (Tomczak and Godfrey, 1994).

The variation in the southern sector's physico-chemical parameters is most marked across the line of the fronts, i.e. approximately longitudinally. Of the nine WOA01 oceanic parameters, temperature, salinity, nitrate, phosphate, and dissolved oxygen down to 1000 m all vary monotonically with respect to latitude (and are, therefore, strongly correlated with one another) at least to about 50° S. It follows that alkalinity [empirically, a second order function of temperature, (Millero et al., 1998)], density (a function

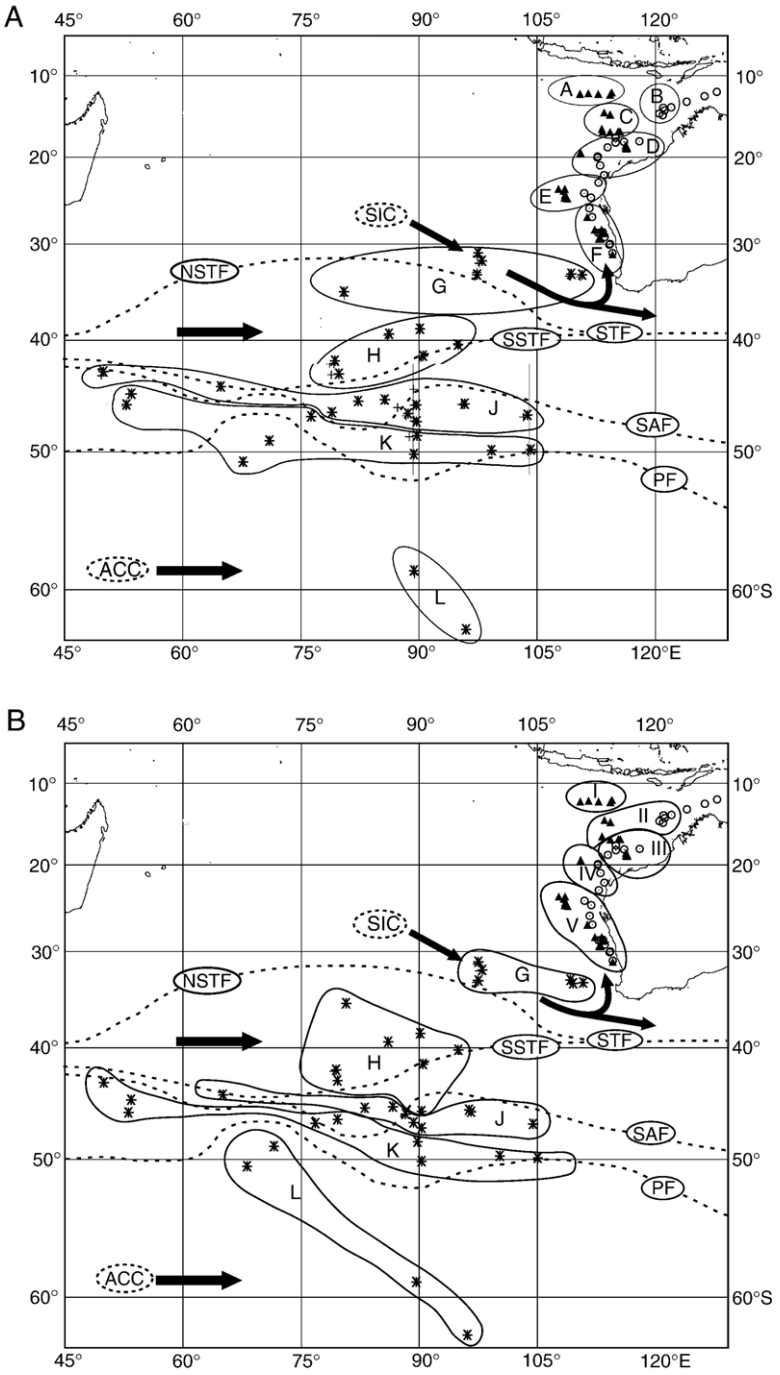

Fig. 1. Locality map of the core tops sampled. Open circles refer to the RV *Franklin* cruise 10-95, triangles to the RV *Franklin* cruise 02-96, and asterisks to various cruises of the RV *Marion Dufresne* I and II between 1988 and 2004. The southern Indian Ocean currents and fronts are shown, as well as the environmental provinces and radiolarian assemblages — abbreviations as follows: Currents — ACC: Antarctic Circumpolar; SIC: South Indian. Fronts — NSTF: Northern Subtropical; SSTF: Southern Subtropical; SAF: Subantarctic; PF: Polar. The fronts are plotted using Belkin and Gordon's (1996) data with the surrounding shading to suggest the seasonal and longer-term fluctuations in their positions. 1A. Boundaries of the environmental provinces labelled A to L, omitting I. 1B. Boundaries of the radiolarian assemblages: the eastern sector assemblages are labelled I to V and the southern assemblages G to L.

of temperature, salinity, and pressure), and P*, where P* is the excess of phosphorus relative to the standard nitrogen quota, i.e. $P^* = [PO_4^{3-}] - [NO_3^-]/16$ (Deutsch et al., 2007), are also strongly correlated with latitude. No other environmental parameter exhibits an obvious pattern.

2.2. The eastern Indian Ocean

The oceanography of the eastern Indian Ocean is complex (Fig. 2). However, it is broadly evident that, north of North West Cape (21.78° S 114.17° E),

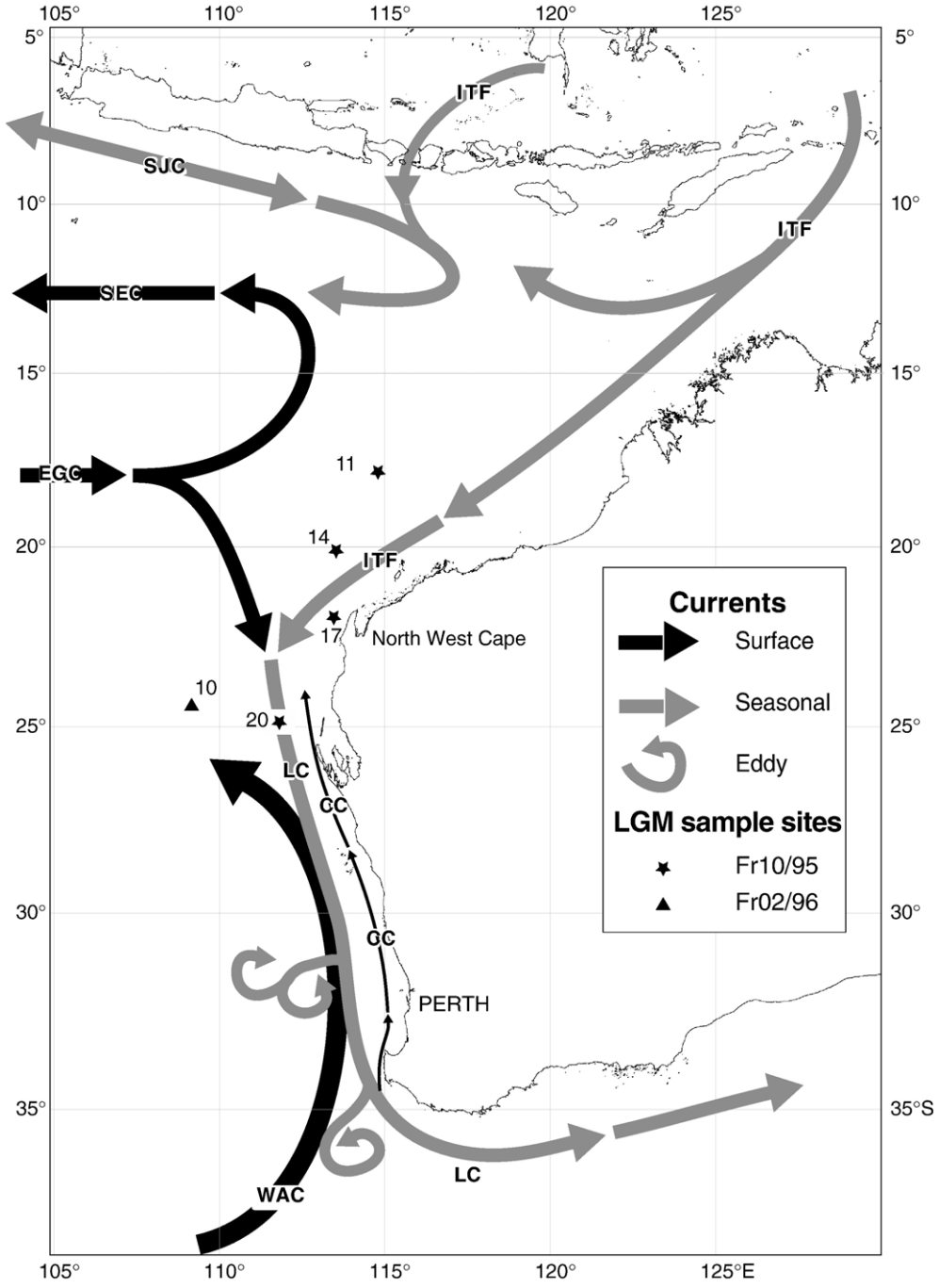

Fig. 2. The LGM fossil sample sites and the currents in the eastern Indian Ocean. SJC: South Java (seasonally reversing); ITF: Indonesian Throughflow; SEC: South Equatorial; EGC: Equatorial Gyral; WAC: Western Australian; LC: Leeuwin; CC: Cape and other coastal currents. (Details and references in text.)

conditions are dominated by the Indonesian Throughflow (ITF) and the South Java Current (SJC). The most important influence for the majority of the study's thirty-two sample sites in this region is the ITF, which, due to its origins in low-latitude waters with high precipitation, is warm, low in salinity, and, hence, of low density. Five of the thirty-two sites [Fr02/96-GC15 to GC19 inclusive — see Table 1] lie at the edge of the Java Upwelling System, an upwelling of high-salinity, low-oxygen, water adjacent to Indonesia (Fieux et al., 1994).

South of North West Cape, the ITF merges with the southwest-flowing component of the Eastern Gyral Current (EGC) to form the Leeuwin Current (LC) which flows generally southward parallel to the Western Australian coast, the merger being accompanied by a sharp rise in salinity (Quadfasel et al., 1996; WOA01, 2001). Flowing in the opposite direction to the LC is the West Australian Current (WAC), the northward leg of the South Indian Ocean Gyre. The WAC forms the western boundary of the LC but, because the WAC is cold and saline and the LC remains relatively warm and fresh (Cresswell and Golding, 1980; Thompson, 1983), the eastern part of the WAC flows under the LC to form the Leeuwin Undercurrent (LUC). At the same time, the LC is constrained to flow as a shallow and narrow band of water, never more than 250 m deep and around 50 km wide (Pearce and Cresswell, 1985; Smith et al., 1991), with its width and course variable, and with eddies which are large relative to the LC itself, particularly along its western (seaward) edge (Pearce, 1991). The LC is separated from the coast by seasonally-reversing coastal currents (Pearce and Pattiaratchi, 1999; Taylor and Pearce, 1999) and, although it flows all year round (Meyers et al., 1995), the LC is stronger in austral winters, especially during La Niña events (Pearce and Phillips, 1988; Cresswell, 1991; Pearce, 1991; Smith et al., 1991; Feng et al., 2003).

The complexity of the currents is reflected in a similar complexity in the oceanic parameters. Temperature is inversely correlated with salinity and density and, less strongly, chlorophyll and dissolved oxygen. The other WOA01 physico-chemical data which might possibly determine radiolarian populations vary in less regular fashion and, a priori, the distribution of taxa might be expected to reflect this irregularity.

3. Materials and methods

3.1. Radiolarian samples

The study started with 98 core tops drawn from a succession of cruises that took place between 1988 and 2004 at the locations listed in Table 1 and shown in Fig. 1. Four samples (Fr10/95-GC1-3 and 28) were omitted from further analysis when they were found to be almost devoid of Radiolaria. The eastern Indian Ocean samples, with one exception, were all taken during two cruises of the RV *Franklin*, Fr10/95 and Fr02/96; the exception coming from an RV *Marion Dufresne* cruise in 2000. The Southern Ocean samples came from RV *Marion Dufresne* I and II cruises in 1988, 1994, 1997, 2002, and 2004.

The RV *Franklin* samples were obtained from gravity cores which do not necessarily return the material from the sediment–water interface. However, our samples may be regarded as the best that it is possible to obtain from gravity cores because Martínez, who used the same samples in his study of planktonic foraminifera (Martínez et al., 1998), took the top of each core onboard ship, as it was recovered, in order to minimise the effects of mixing. The RV *Marion Dufresne* samples comprise a mixture of short-trigger, box, gravity, and piston cores.

3.2. Oceanographic data

The World Ocean Atlas 2001 (WOA01, 2001) contains objectively analysed data for sea temperature, salinity, dissolved oxygen, apparent oxygen utilisation, percentage oxygen saturation, phosphate, nitrate, silicate, and chlorophyll concentrations at a selection of depths down to 5500 m on annual, seasonal, and monthly timescales. The initial environmental dataset for our study consisted of the annual, and the austral spring (October to December), summer (January to March), autumn (April to June), and winter (July to September), values, where available, for each of the nine parameters at each site at the surface and depths of 20, 50, 75, 100, 150, 200, 250, 300, and 500 m. To these data were added values for four derivative parameters: water density (Schlitzer, 2005), P* (Deutsch et al., 2007), Si*, an indicator of nutrient status related to the requirements of diatoms, and thus, probably, radiolarians, where $Si^* = [Si(OH)_4] - [NO_3^-]$ (Sarmiento et al., 2004), and salinity-normalised total alkalinity (NTA — Millero et al., 1998) — the last at the sea-surface only because it is defined as a function of SST. The site values were derived from the WOA01 1° latitude by 1° longitude grid using linear interpolation.

3.3. Laboratory methods

In order to dissolve any carbonates present, samples for the study (which came from the uppermost 1–2 cm of each core) were digested with 10% hydrochloric acid until no further effervescence was evident. In the few cases, when this process did not also cause the clays to disaggregate

Table 1
Sample site locations and associated parameters in latitude order

Core [cruise-core]	Latitude [° S]	Longitude [° E]	Depth bsl. [m]	Assemblage	WADE	URI
Fr10/95-GC01	12° 00.00′	127° 50.00′	124	na	na	na
Fr02/96-GC18	12° 05.17′	114° 27.24′	3189	A01	7.90	0.80
Fr02/96-GC16	12° 11.29′	111° 30.45′	2714	A02	3.82	0.00
Fr02/96-GC15	12° 14.41′	110° 25.70′	3446	A03	5.30	0.00
Fr02/96-GC17	12° 14.80′	112° 44.27′	2571	A04	8.14	0.00
Fr02/96-GC19	12° 22.76′	114° 16.96′	3355	A05	5.18	0.00
Fr10/95-GC02	12° 32.86′	126° 14.84′	80	na	na	na
Fr10/95-GC03	13° 14.53′	124° 00.23′	182	na	na	na
Fr10/95-GC04	13° 55.18′	122° 01.51′	470	B01	43.67	0.00
Fr10/95-GC05	14° 00.55′	121° 01.58′	2472	B02	3.03	0.00
Fr10/95-GC06	14° 19.67′	121° 09.81′	2177	B03	12.11	2.05
Fr02/96-GC20	14° 34.95′	113° 30.49′	2497	C01	8.05	0.00
Fr10/95-GC07	14° 42.58′	120° 32.74′	1440	B04	2.05	9.62
Fr02/96-GC21	14° 48.68′	114° 16.37′	2919	C02	6.86	0.48
Fr10/95-GC08	14° 54.97′	120° 57.49′	625	B05	12.09	1.12
Fr02/96-GC22	16° 34.71′	113° 11.98′	2501	C03	5.73	0.00
Fr02/96-GC26	16° 54.00′	115° 31.00′	1958	C04	9.90	1.38
Fr02/96-GC25	16° 54.65′	115° 15.90′	1666	C05	5.58	0.00
Fr02/96-GC23	16° 54.81′	113° 20.14′	1987	C06	26.50	0.00
Fr02/96-GC24	16° 55.61′	114° 15.46′	1603	C07	12.33	0.00
Fr10/95-GC11	17° 38.57′	114° 59.93′	2458	C08	7.82	0.53
Fr10/95-GC09	18° 07.63′	118° 00.92′	498	C09	114.00	0.00
Fr10/95-GC10	18° 08.93′	116° 01.32′	1462	C10	17.62	1.38
Fr10/95-GC12	18° 14.70′	114° 59.63′	2034	C11	3.73	2.56
Fr02/96-GC27	18° 33.71′	116° 16.01′	1024	C12	6.25	0.00
Fr02/96-GC28	18° 47.93′	116° 20.23′	502	C13	0.00	0.00
Fr10/95-GC13	18° 49.26′	113° 58.44′	1454	C14	17.10	0.00
Fr02/96-GC29	18° 57.81′	116° 23.52′	344	C15	28.00	0.00
Fr02/96-GC14	19° 24.64′	110° 30.40′	4090	D01	6.36	1.49
Fr10/95-GC14	20° 02.71′	112° 39.73′	997	D02	53.50	0.74
Fr10/95-GC16	20° 59.83′	112° 59.35′	1221	D03	20.20	0.00
MD00-2361	22° 04.92′	113° 28.63′	1805	D04	4.97	0.77
Fr10/95-GC17	22° 07.74′	113° 30.11′	1093	D05	5.69	0.00
Fr10/95-GC18	22° 59.64′	112° 49.86′	1055	D06	4.62	3.12
Fr02/96-GC13	23° 43.75′	107° 42.71′	3189	E01	1.50	0.00
Fr02/96-GC11	23° 57.16′	108° 22.14′	2404	E02	9.80	0.00
Fr10/95-GC19	24° 14.11′	111° 00.18′	1974	E03	8.22	0.91
Fr02/96-GC10	24° 27.85′	108° 30.61′	2852	E04	13.07	0.41
Fr10/95-GC20	24° 44.67′	111° 49.75′	837	E05	27.40	0.00
Fr02/96-GC09	24° 44.83′	108° 29.26′	2534	E06	18.33	3.49
Fr02/96-GC08	24° 50.76′	108° 49.48′	2670	E07	1.90	0.00
Fr10/95-GC21	25° 59.78′	111° 38.09′	982	F01	0.25	0.00
Fr02/96-GC07	26° 58.76′	111° 20.13′	3090	F02	8.82	1.77
Fr10/95-GC22	26° 59.52′	112° 00.31′	1049	F03	26.00	1.08
Fr02/96-GC05	28° 23.55′	113° 09.57′	735	F04	11.88	0.00
Fr02/96-GC06	28° 25.21′	112° 17.37′	3575	F05	0.00	0.00
Fr02/96-GC04	28° 43.02′	113° 23.32′	936	F06	16.75	2.11
Fr10/95-GC25	28° 43.93′	113° 22.08′	1010	F07	16.50	2.04
Fr10/95-GC23	28° 44.70′	112° 46.94′	2470	F08	20.00	0.00
Fr10/95-GC24	28° 45.04′	113° 03.87′	1577	F09	5.64	0.00
Fr10/95-GC26	29° 14.42′	113° 33.48′	1734	F10	4.17	1.18
Fr02/96-GC03	29° 17.78′	112° 56.58′	3343	F11	4.50	0.00
Fr02/96-GC02	29° 20.95′	112° 56.91′	3377	F12	11.00	0.00
Fr10/95-GC27	30° 00.14′	114° 16.64′	853	F13	9.50	0.00
Fr10/95-GC28	30° 04.88′	114° 08.51′	1440	F14	2.50	0.00
Fr10/95-GC29	30° 59.51′	114° 35.37′	1200	F15	5.50	1.43
Fr02/96-GC01	31° 06.64′	114° 32.89′	2530	F16	5.53	0.64

Table 1 (*continued*)

Core [cruise-core]	Latitude [° S]	Longitude [° E]	Depth bsl. [m]	Assemblage	WADE	URI
MD94-117	31° 37.00′	97° 42.83′	2360	G01	1.75	7.55
MD94-10B	32° 09.87′	97° 41.74′	1660	G02	0.89	0.93
MD94-115	33° 10.81′	97° 36.75′	4020	G03	1.00	0.00
MD94-12B	33° 31.70′	109° 09.00′	4110	G05	2.62	1.14
MD94-13B	33° 32.45′	109° 18.48′	3560	G06	2.41	5.60
MD94-11B	33° 34.71′	110° 35.09′	2400	G07	5.08	0.00
MD94-09B	33° 35.43′	97° 35.87′	4185	G04	1.13	1.60
MD97-2100	35° 57.85′	80° 55.72′	2510	H01	0.82	0.00
MD94-08B	38° 51.82′	90° 06.10′	3491	H02	1.08	0.71
MD97-2102	39° 55.25′	86° 00.41′	3440	H03	1.73	0.00
MD94-113	40° 40.30′	94° 81.30′	3436	H04	0.80	0.00
MD94-07B	41° 43.20′	90° 16.71′	2768	H05	1.14	0.53
MD94-01B	42° 30.00′	79° 25.00′	2920	H06	4.25	0.00
MD02-2483	43° 23.60′	49° 47.30′	2300	K01	0.04	2.42
MD04-2714	43° 23.90′	49° 49.20′	2300	K02	0.32	0.00
MD97-2101	43° 29.74′	79° 50.30′	3145	H07	1.00	0.00
MD94-102	43° 30.34′	79° 50.18′	3205	H08	1.50	0.00
MD88-764	44° 24.08′	65° 08.03′	4530	J01	2.56	0.00
MD94-06B	44° 39.90′	90° 04.55′	3315	H09	1.37	0.00
MD02-2484	45° 04.60′	53° 19.80′	3400	K03	0.09	0.00
MD94-02B	45° 35.22′	86° 31.00′	3205	J02	0.69	1.49
MD88-768	45° 45.19′	82° 55.69′	3330	J03	0.41	0.00
MD88-770	46° 01.32′	96° 27.64′	3290	J05	0.44	0.24
MD97-2104	46° 02.23′	96° 29.00′	3310	J04	0.39	1.57
MD88-769	46° 04.16′	90° 06.67′	3420	H10	1.32	0.00
MD04-2716	46° 09.90′	52° 55.60′	3320	K04	0.08	0.00
MD94-104	46° 28.97′	88° 04.16′	3460	J06	0.29	1.04
MD88-766	46° 38.79′	79° 28.22′	2920	K05	0.24	0.90
MD88-767	46° 40.01′	79° 30.05′	2930	K06	0.26	0.46
MD02-2486	47° 00.20′	89° 06.70′	3380	J07	1.04	0.58
MD88-765	47° 01.26′	76° 55.96′	3420	K07	0.38	0.00
MD97-2105	47° 11.58′	104° 28.57′	3300	J08	0.41	0.00
MD94-107	47° 46.17′	90° 14.21′	3525	J09	0.24	1.83
MD94-05B	48° 48.08′	89° 32.48′	3730	K08	0.16	0.39
MD04-2720	49° 07.60′	71° 22.10′	750	L01	0.02	0.00
MD88-771	49° 55.26′	100° 06.72′	3310	K09	0.10	2.24
MD88-772	50° 01.35′	104° 53.81′	3240	K10	0.04	0.00
MD94-04B	50° 22.85′	90° 15.16′	4036	K11	0.28	0.00
MD88-795	50° 50.56′	68° 01.08′	1870	L02	0.10	0.00
MD88-794	58° 59.52′	89° 24.14′	4595	L03	0.32	0.00
MD88-793	62° 29.40′	95° 55.94′	3790	L04	0.61	2.24

Assemblage membership is indicated by the initial letter of the trigraph under the heading "Assemblage". na = not available; bsl. = below sea level.

completely, the samples were further treated with 3% hydrogen peroxide and placed in a gentle ultrasound bath for approximately 20 seconds. Sampling indicated that neither the hydrogen peroxide treatment nor the ultrasound had any adverse effects on the radiolarian tests but, as a precaution, these treatments were avoided as far as possible. Once all the unwanted material was fully digested or disaggregated, samples were washed through a 63 μm sieve with a gentle water jet and the coarse fraction transferred to vials. After being allowed to settle at least overnight, as much water as it was possible to decant from the vials without loss of Radiolaria was removed by pipetting and replaced with ethanol. This process was repeated twice more to maximise the replacement of water. Then, residue samples were mounted on slides for microscopic examination, using Naphrax® as the mount-medium.

The amount of residue transferred to a slide was intended to ensure there were at least 300 radiolarian tests to count for each core top, a number chosen to reduce to less than 1% the probability of failing to detect any taxon which comprised at least 1% of the population (see Fatela and Taborda, 2002). When necessary, several slides were made from the same sample in an attempt to

obtain the 300 specimens. The slides were examined at a magnification of 100 or higher when identification proved more difficult. Taxa assignments were primarily made using the descriptions and photographs appearing in Dolven (2004), assisted by reference to three other online databases (Nigrini and Moore, 1979; Boltovskoy, 1998; Nigrini et al., 2004). The photographs in van de Paverd's (1995) PhD thesis often provided initial identification but were only used for taxa assignment as a last resort because van de Paverd's classification proposals have not yet been peer-reviewed.

4. Results

4.1. Data details

An average of 487 Radiolaria per core top were counted, yielding a database of some 50,000 specimens: 281 taxa were observed, an average of 59 per core top. The senior author could not identify every specimen to a specific species or genus and, to avoid the errors this might introduce, taxonomic groups of doubtful homogeneity were removed from the data for statistical analysis, as were the rarest species (<10 specimens observed or <5 in at least one sample), and the core tops with very few radiolarian specimens (<100). In fact, because the weighted averaging (WA) methods proved the most suitable for palaeoreconstruction, the removal of the rarer species served little purpose other than to ease data-handling. Birks (1994) established that, using WA, the inclusion of the rarer species was beneficial or neutral in effect because species' absences are ignored in WA regression. Some analyses of our data were performed both with and without the rarer species and the results found to differ only marginally, tending to confirm Birks' (1994) conclusions. Our criteria for the deletion of sites and species resulted in the exclusion of six sites — Fr10/95-GC 21 and 27, Fr02/96-GC 2, 6, and 13, and MD94-115. The resultant dataset (the *radiolarian data*) was the basis for all further analysis.

A full species list and the radiolarian abundance counts are available as an electronic supplement to this paper and in BLUENET, the Australian Marine Science Data Network (www.bluenet.org.au). A list of the *Indicator Species* (see Section 4.3. below) appears as Table 2 with photographs as Figs. 3 and 4. Photographs of all the identified species will be submitted to the online database radiolaria.org (Dolven, 2004) as they become available.

4.2. Determination of radiolarian assemblages

Statistical analysis, mainly using the "R" statistical computing software (R Development Core Team, 2004), was performed on the eastern and southern Indian Ocean data separately, as well as with the two sectors combined. Because the samples varied in numbers of specimens they contained, the species counts for each sample were first reduced to percentages of the site totals. Agglomerative hierarchical cluster analysis [AHCA — *R* software's *hclust* (Murtagh)] on the combined data using average-linkage clustering with Bray–Curtis distances gave a cophenetic correlation index (CCI) of 0.88. This analysis revealed clear separations between those sites in the eastern sector and those in the southern sector and between those southern sites lying north of the Southern Subtropical Front (SSTF) and those to the south of that front. Less strongly, the southern sector shows evidence of five sub-clusters of geographically proximate sites.

Multivariate regression trees (MVRT) [*R's mvpart* (Breiman et al., 1984; De'ath, 2002)], which are, in effect, constrained cluster analyses, were used to relate the radiolarian data clusters to the environmental data. An MVRT applied to the combined data supported the existence of around ten radiolarian assemblages, principally associated with temperature and salinity. An MVRT of the southern sector data alone reinforced the credibility of the five assemblages found in the combined data AHCA. An AHCA on the southern sector environmental data also gave five assemblages (CCI=0.80): these assemblages are very similar to the MRVT set. Both the AHCA and the MVRT assemblages have been labelled from north to south as G to L (omitting "I" to avoid confusion) (Fig. 1).

MRVT evidence for the eastern sector was less clear: temperature and salinity seemed to be the main determining factors and five assemblages were apparent (labelled I–V in Fig. 1B). AHCA of the radiolarian data produced no credible results. However, an AHCA of the corresponding environmental data suggested six sectors (CCI=0.88), and this broadly corresponded to the MVRT. The six environmental sectors have been labelled A to F (Fig. 1A). Confidence in these and the southern sector assemblages was enhanced by the application of Canonical Variance Analysis (CVA) (Hammer et al., 2001; Hammer and Harper, 2006) to the radiolarian dataset (Fig. 5).

The Upwelling Radiolarian Index (URI) (Nigrini and Caulet, 1992) and the Water Depth Ecology index (WADE) (Lazarus et al., 2006) were calculated for each site ("WADE" and "URI" respectively in Table 1). The definition of the taxa observed in our study as *warm*, *temperate*, *intermediate*, or *upwelling* was drawn from Lazarus et al. (2006). Fifty-two of the 62 taxa classified by these authors are represented amongst the 281 taxa of our study.

Table 2
List of *indicator species*

Indicator species		Probability of indicator values		
Figure	Taxon	ES (≤0.04)	SS (≤0.003)	E and SS (≤0.003)
3-A	*Acanthodesmia vinculata* (Müller) 1858	0.03	0.001	0.003
3-J	*Acrosphaera spinosa* (Haeckel) 1861	0.04	0.001	
3-F	*Actinomma antarcticum* (Haeckel) 1887			0.002
3-H	*Actinomma hastatum* (Haeckel) 1887			0.001
3-O	*Antarctissa* spp. Petrushevskaya 1975		0.001	0.001
3-N	*Botryocyrtis scutum* (Harting) 1863	0.01		
3-K	*Cenosphaera* sp in det Benson 2003	0.02		0.001
3-C	*Collosphaera huxleyi* Müller 1855			
3-B	*Collosphaera tuberosa* (Haeckel 1887) Nigrini 1971		0.001	
3-L	*Cycladophora bicornis* (Popofsky) Lombari and Lazarus 1988		0.001	0.001
3-Q	*Cycladophora davisiana* Ehrenberg 1862			0.003
3-I	*Cypassis irregularis* Nigrini 1968	0.01		
3-M	*Didymocyrtis tetrathalamus* (Haeckel) 1887		0.001	
3-G	*Euchitonia triangulum* (Ehrenberg) 1872	0.01		0.002
3-E	*Hexastylus dimensivus* Haeckel 1887	0.03		
3-P	*Lamprocyclas maritalis maritalis*		0.001	0.001
3-R	*Lamprocyclas maritalis polypora* Nigrini 1967		0.003	0.001
3-D	*Lophophaena hispida* (Ehrenberg) 1872		0.001	0.001
4-A	*Phormospyris stabilis antarctica* (Haeckel) (Goll 1974)			0.002
4-B	*Polysolenia lappacea* (Haeckel) Nigrini 1967	0.03	0.001	
4-G	*Saccospyris antarctica* Haecker 1907		0.001	0.001
4-M	*Siphonosphaera polysiphonia* Haeckel 1887–Nigrini 1967		0.001	
4-I	*Sphaerozoum punctatum* Müller 1858		0.002	
4-L	*Spongaster tetras* Ehrenberg 1860	0.02		
4-O	*Spongodiscus* spp. Ehrenberg 1854	0.01		
4-N	*Spongopyle osculosa* Dreyer 1889			0.002
4-F	*Spongotrochus glacialis* Popofsky 1908		0.001	
4-E	*Spongurus ellipticus* Ehrenberg 1872	0.04		
4-C	*Stylodictya aculeata* Jørgensen 1905	0.02		
4-K	*Stylosphaera* sp aff. *S. hispida* Ehrenberg 1854	0.00	0.002	0.002
4-J	*Tetrapyle octacantha* group Müller 1858	0.01	0.003	0.003
4-D	*Theocorythium trachelium* Ehrenberg 1872	0.02		0.002
4-H	*Tholospironium cervicorne* Haeckel 1887	0.05		

The entry under "Sector" group specifies in which Indian Ocean sector the taxon is significant and to what extent. ES = Eastern sector; SS = Southern sector; E and SS = Eastern and southern sectors combined.

4.3. Isolation of explanatory environmental variables

Correspondence Analysis (CA) [*R's cca*(Legendre and Legendre, 1998)] was applied to the combined radiolarian data and the sites scores correlated with the environmental data. Spearman correlation coefficients greater than 0.8 (87 degrees of freedom, probability $< 10^{-20}$) were obtained for temperatures for all four seasons and at all depths from the surface to 300 m with the highest correlations (coefficients >0.85) at depths of 150 and 200 m. The correlations with austral winter concentrations of nitrate and phosphate at depths between 20 and 75 m are similarly strong, as is the correlation with alkalinity for all seasons. The first CA eigenvalue was 2.4 times the size of the second and the first eigenvalue of a detrended correspondence analysis (DCA) of the same data [*R's decorana* (Hill, 1980)] gave a first eigenvalue 4.9 times the second. These results indicate that only one environmental variable (or a set of collinear variables) determined the distribution of radiolarian taxa.

All nine WOA01 parameters and their four derivatives (NTA, density, P*, and Si*) were employed in turn as the constraining variable in a Canonical Correspondence Analysis (CCA) of the radiolarian data and the proportion of the taxa variance explained by that environmental variable calculated by dividing the constrained inertia by the total inertia [*R's cca* (Jongman et al., 1987; ter Braak and Verdonschot, 1995; Legendre and Legendre, 1998)]. NTA at the sea-surface, temperature from the surface to 300 m, and nitrate, phosphate,

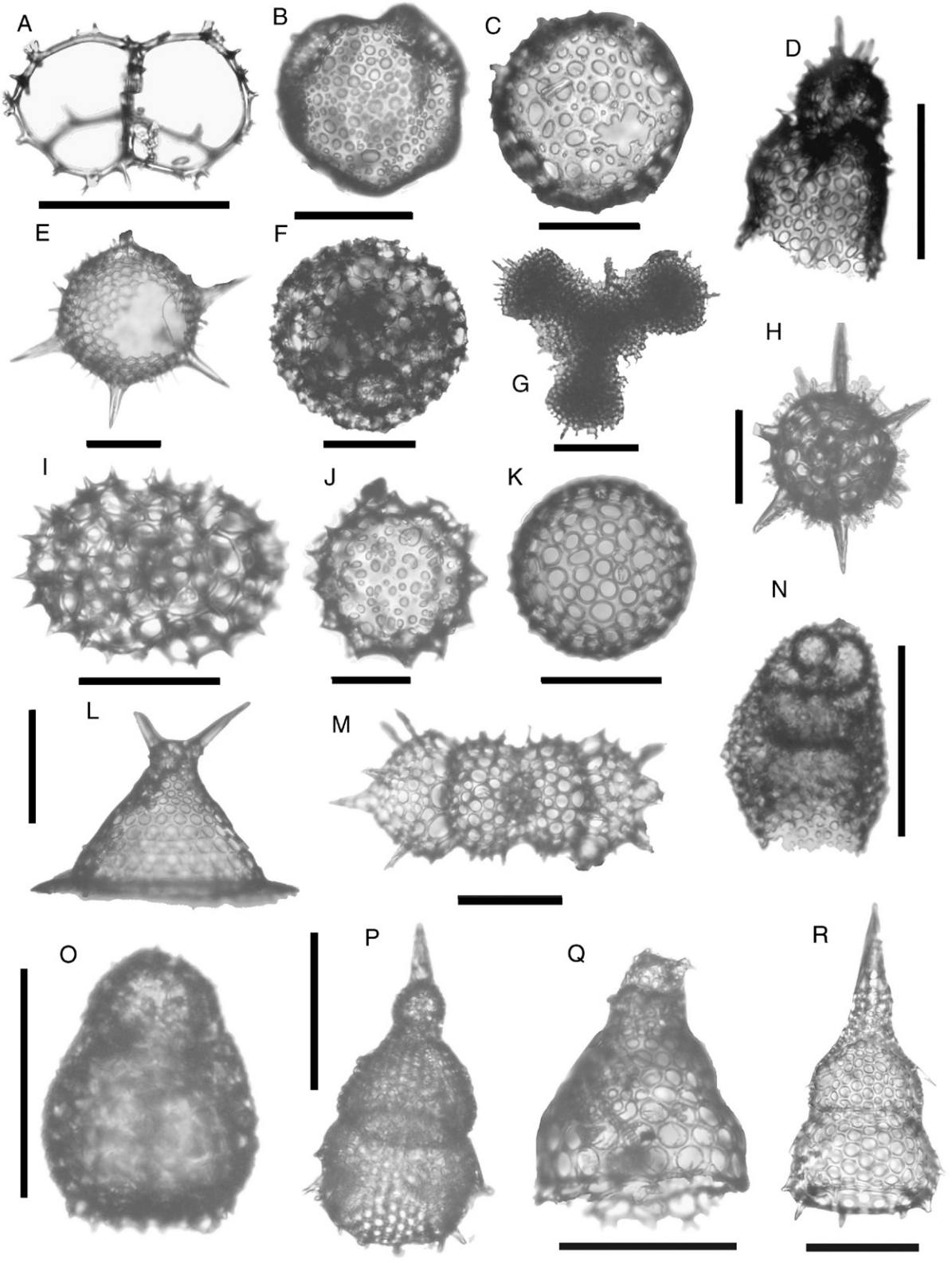

Fig. 3. Indicator species — part 1. Key in Table 2; size bars 100 μm.

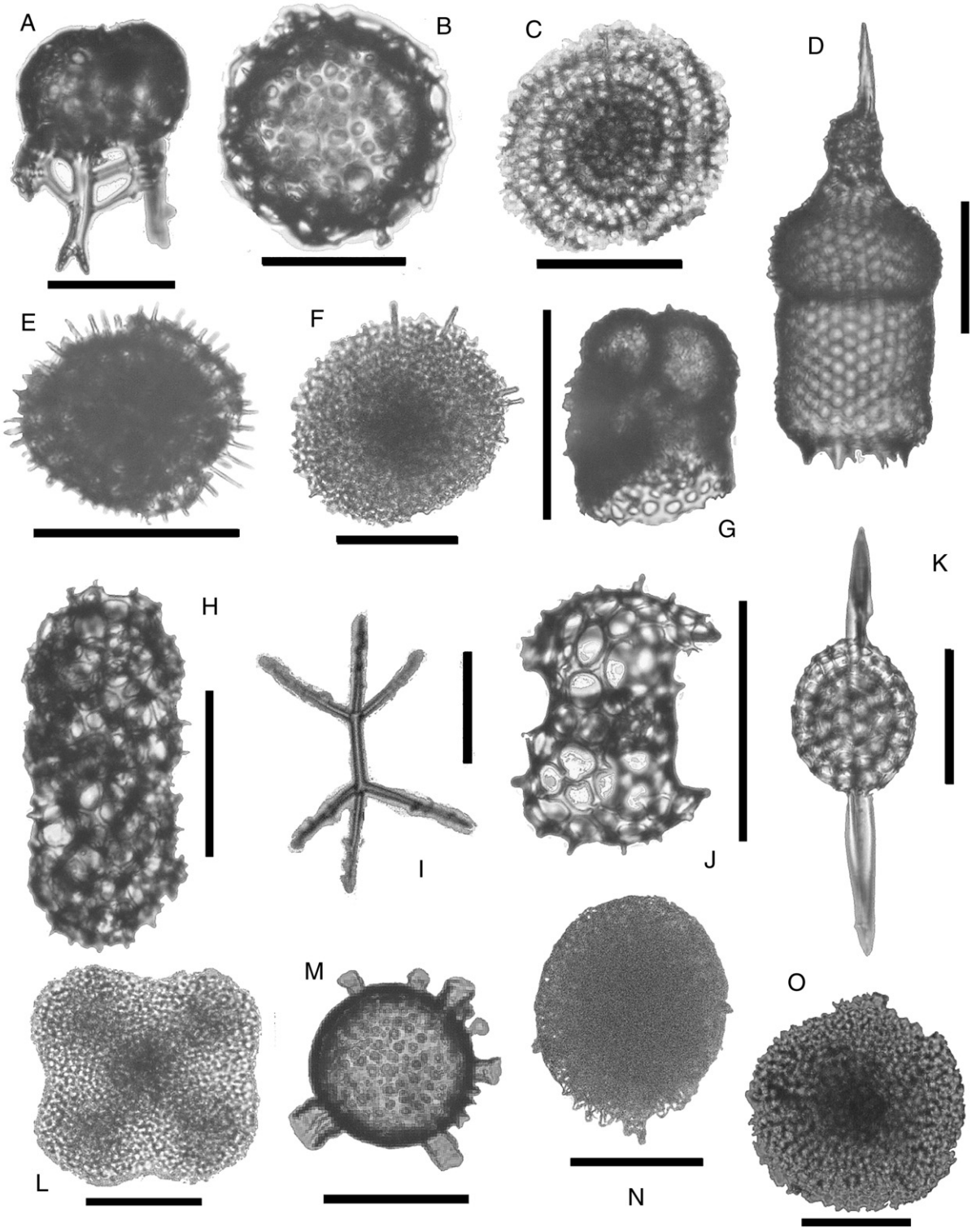

Fig. 4. Indicator species — part 2. Key in Table 2; size bars 100 μm.

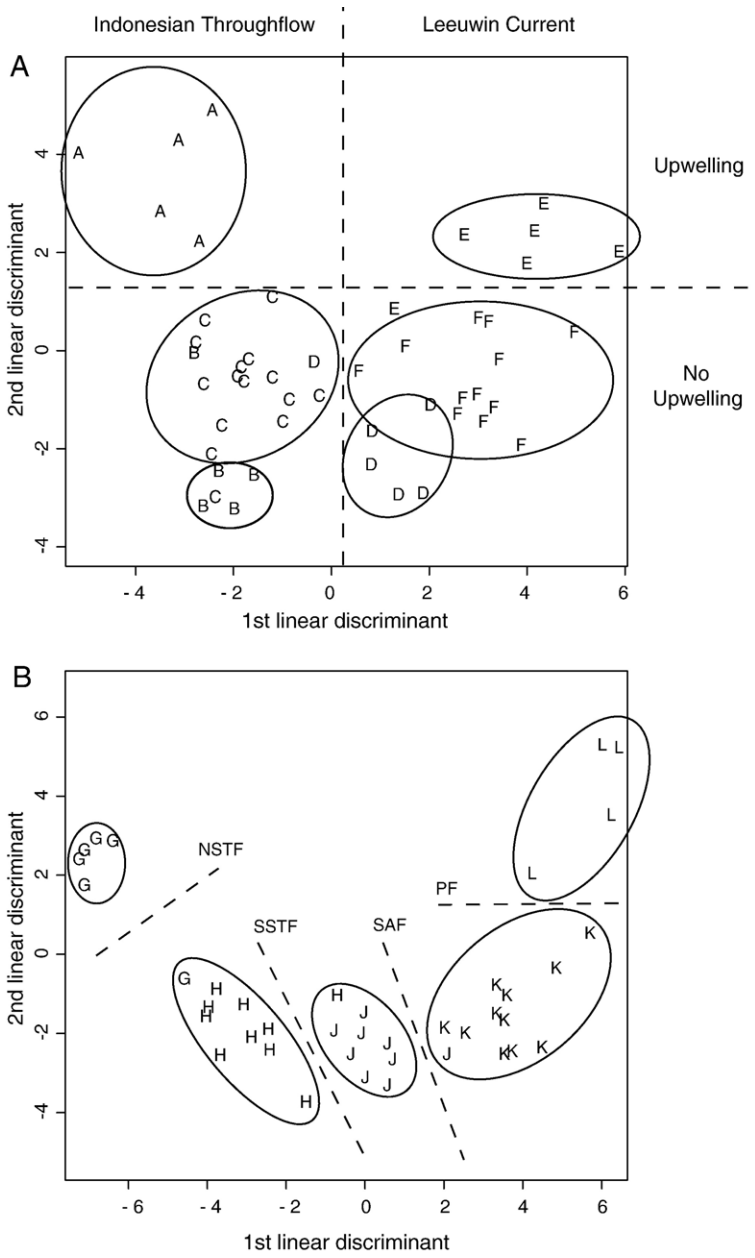

Fig. 5. CVA applied to the radiolarian data grouped in accordance with their environmental provinces: first discriminant plotted against the second; sample points represented by the letter indicating their assemblage (Table 1). A: Eastern sector — the assemblages correspond well with the interactions of the sector's currents (abbreviations as in Fig. 2) — A: Java Upwelling area; B: ITF; C: confluence of the SJC, the EGC and the ITF; D: the southern ITF; E: the confluence of the EGC and ITF; F: the LC and the LUC. B: Southern sector — broadly, assemblage G lies north of the NSTF, H between the NSTF and the SSTF, J between the SSTF and the SAF, K between the SAF and the PF, and L south of the PF (abbreviations as in Fig. 1).

and dissolved oxygen from the surface to 100 m each explained 25% to 29% of the taxa variance both on an annual basis and for each of the four seasons (Fig. 6 and electronic supplement). Density explained in excess of 20% of the variance at all depths to 500 m. The constrained CCA eigenvalues for these variables exceeded 90% of the first CA eigenvalue, indicating that no explanatory variables had been missed. Repeating the CCA using only the radiolarian *Indicator Species* established using the Dufrêne-Legendre (1997) technique raised the taxa variance explained by each of the variables over the same depths to over 43%.

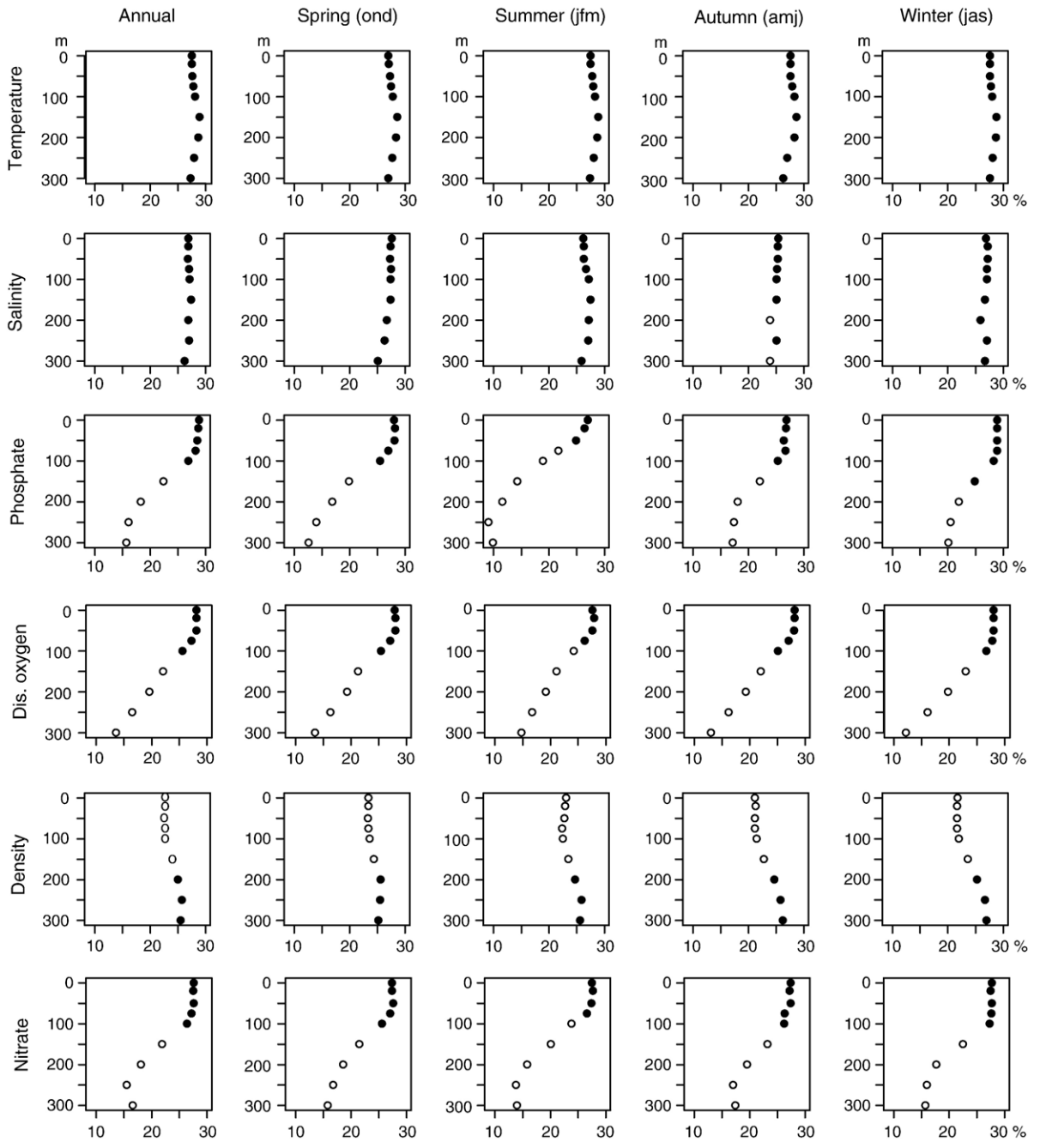

Fig. 6. Percentage of taxa variance explained by the main environmental variables (annual, austral spring, summer, autumn, and winter) at depths between the sea-surface and 300 m. The results for temperature, phosphate, dissolved oxygen, density, and nitrate are based on the radiolarian data from the eastern and southern sectors combined; the salinity results come from the southern sector alone. Filled circles indicate explained variance values >24.5%.

CCA on the southern sector data, using the individual environmental variables in turn, yielded similar results to those for the combined data except in that salinity at depths from the surface down to 300 m accounted for 24% to 28% of the taxa variance for every season as compared to 16% to 19% for the combined data.

The forty-nine eastern sector sites were subjected to the same statistical analysis as applied to the southern and the

Table 3
Last glacial maximum SST reconstructions

Sector(s)	Regression and calibration method	Core	Depth in core (cm)	SST estimates ± 1 standard error [°C]			Differences from Barrows and Juggins (2005) [°C]		
				Annual	Summer	Winter	T_{mean}	T_{max}	T_{min}
Combined eastern and southern sectors	WA inverse deshrinking	Fr10/95-GC11	27	23.3±0.4	24.7±0.4	21.4±0.5	−1.0	−2.0	−0.8
		Fr10/95-GC14	45	25.0±0.3	26.5±0.3	23.4±0.3	3.3	2.6	3.8
		Fr10/95-GC17	127	23.4±0.3	24.8±0.3	21.7±0.4	2.0	1.1	2.1
		Fr10/95-GC20	54	25.0±0.4	26.5±0.4	23.4±0.3	3.3	2.6	3.6
		Fr02/96-GC10	20	21.7±0.4	23.1±0.4	20.1±0.4	−0.2	−0.9	0.2
		Fr02/96-GC10	22	23.3±0.4	24.6±0.4	21.3±0.4	1.4	0.6	1.4
	WA-PLS	Fr10/95-GC11	27	**24.5±0.7**	**26.0±0.7**	**22.6±0.7**	**0.2**	**−0.7**	**0.4**
		Fr10/95-GC14	45	**23.4±0.5**	**25.0±0.6**	**21.6±0.4**	**1.7**	**1.1**	**2.0**
		Fr10/95-GC17	127	**24.3±0.5**	**26.0±0.6**	**22.3±0.4**	**2.9**	**2.3**	**2.7**
		Fr10/95-GC20	54	**20.8±0.7**	**22.7±0.9**	**19.1±0.6**	**−0.9**	**−1.2**	**−0.7**
		Fr02/96-GC10	20	**21.3±0.7**	**22.7±0.7**	**19.6±0.6**	**−0.6**	**−1.3**	**−0.3**
		Fr02/96-GC10	22	**22.3±0.6**	**23.8±0.7**	**20.6±0.6**	**0.4**	**−0.2**	**0.7**
	MAT	Fr10/95-GC11	27	26.6±0.6	28.3±0.6	24.5±0.5	2.3	1.6	2.3
		Fr10/95-GC14	45	24.8±0.8	26.4±0.9	23.1±0.7	3.1	2.5	3.5
		Fr10/95-GC17	127	26.2±0.7	27.7±0.7	24.3±0.6	4.8	4.0	4.7
		Fr10/95-GC20	54	23.0±0.8	24.4±1.0	21.5±0.7	1.3	0.5	1.7
		Fr02/96-GC10	20	25.3±1.4	26.8±1.5	23.5±1.4	3.4	2.8	3.6
		Fr02/96-GC10	22	24.6±0.9	26.1±1.0	22.9±0.8	2.7	2.1	3.0
	Maximum likelihood	Fr10/95-GC11	27	26.8±0.5	28.4±0.5	24.7±0.5	2.5	1.7	2.5
		Fr10/95-GC14	45	23.8±0.5	25.3±0.5	22.2±0.4	2.1	1.4	2.6
		Fr10/95-GC17	127	24.5±0.8	26.4±1.0	22.6±0.9	3.1	2.7	3.0
		Fr10/95-GC20	54	22.6±0.6	24.1±0.5	21.0±0.5	0.9	0.2	1.2
		Fr02/96-GC10	20	22.4±1.0	23.9±1.0	20.9±1.0	0.5	−0.1	1.0
		Fr02/96-GC10	22	24.1±0.8	25.8±1.0	22.3±0.7	2.2	1.8	2.4
Eastern sector	WA inverse deshrinking	Fr10/95-GC11	27	27.5±0.5	29.1±0.5	25.5±0.5	3.2	2.4	3.3
		Fr10/95-GC14	45	23.1±0.5	24.6±0.5	21.5±0.5	1.4	0.7	1.9
		Fr10/95-GC17	127	26.0±0.7	27.5±0.7	24.0±0.6	4.6	3.8	4.4
		Fr10/95-GC20	54	20.5±0.7	22.0±0.8	19.0±0.7	−1.2	−1.9	−0.8
		Fr02/96-GC10	20	26.0±0.4	27.4±0.4	24.2±0.4	4.1	3.4	4.3
		Fr02/96-GC10	22	25.1±0.5	26.6±0.5	23.3±0.5	3.2	2.6	3.4
	WA-PLS	Fr10/95-GC11	27	27.1±0.5	28.8±0.5	25.0±0.5	2.8	2.1	2.8
		Fr10/95-GC14	45	23.8±0.5	25.3±0.5	22.1±0.5	2.1	1.4	2.5
		Fr10/95-GC17	127	25.5±0.7	27.0±0.7	23.5±0.6	4.1	3.3	3.9
		Fr10/95-GC20	54	20.8±0.7	22.3±0.7	19.3±0.6	−0.9	−1.6	−0.5
		Fr02/96-GC10	20	25.5±0.5	26.9±0.5	23.7±0.4	3.6	2.9	3.8
		Fr02/96-GC10	22	24.3±0.5	25.8±0.5	22.5±0.5	2.4	1.8	2.6
	MAT	Fr10/95-GC11	27	25.9±0.6	27.5±0.7	24.0±0.5	1.6	0.8	1.8
		Fr10/95-GC14	45	24.8±0.8	26.4±0.9	23.1±0.7	3.1	2.5	3.5
		Fr10/95-GC17	127	26.2±0.7	27.7±0.7	24.3±0.6	4.8	4.0	4.7
		Fr10/95-GC20	54	23.0±0.8	24.4±0.9	21.5±0.7	1.3	0.5	1.7
		Fr02/96-GC10	20	25.3±1.0	26.8±1.0	23.5±0.8	3.4	2.8	3.6
		Fr02/96-GC10	22	24.6±1.0	26.1±1.1	22.9±0.8	2.7	2.1	3.0
	Maximum likelihood	Fr10/95-GC11	27	17.1±2.4	28.6±0.4	24.9±0.5	−7.2	1.9	2.7
		Fr10/95-GC14	45	19.2±0.3	24.7±1.2	21.9±0.5	−2.5	0.8	2.3
		Fr10/95-GC17	127	17.4±1.9	27.7±0.6	24.0± ±0.7	−4.0	4.0	4.4
		Fr10/95-GC20	54	19.8±0.3	24.2±0.6	21.5±0.4	−1.9	0.3	1.7
		Fr02/96-GC10	20	17.2±2.2	27.6±0.5	24.4±0.6	−4.7	3.6	4.5
		Fr02/96-GC10	22	17.6±2.0	27.5±0.6	23.5±0.8	−4.3	3.5	3.6

Weighted average-partial least squares (WA-PLS) results, which are considered the most reliable overall, are in bold.

combined data. The correlations between the CA scores and the environmental data were considerably weaker than those for the combined or the southern sector data. Despite this, the surface and 50 m values for dissolved oxygen, salinity, and temperature had Spearman coefficients outside the range ±0.77 (37 degrees of freedom,

probability $< 10^{-10}$). The ratios, one to the next, of the first four CA eigenvalues were small, suggesting a multiplicity of explanatory variables. Under CCA, dissolved oxygen (from the surface to 500 m), salinity (from the surface to 200 m), and temperature (from the surface to 100 m) explained approximately 10% of the taxa variance, as did apparent oxygen utilisation, percentage oxygen saturation, and nitrate and phosphate concentrations, all from 75 to 500 m depth. When surface values for dissolved oxygen, salinity, and temperature were used in combination as CCA constraints, they explained only 22% of the taxa variance as compared with 45% when the major explanatory variables were used in CCA on the southern sector data and 42% when applied to the two sectors combined.

4.4. Palaeoenvironmental reconstructions

Fossil samples dated to the LGM were taken from six of the study's eastern Indian Ocean cores whose chronologies were established by Martínez et al. (1999) from the *Globigerinoides sacculifer* $\delta^{18}O$ record. The six cores were selected because they had also been used by Barrows and Juggins (2005) for the estimation of LGM SSTs from the faunal analyses of planktonic foraminifera. The sample from Fr10/95-GC29 yielded virtually no Radiolaria but, because two samples had been taken from adjacent depths (20–21 cm and 22–23 cm) in Fr02/96-GC10, six fossil samples were available for analysis. The location of the sample sites are indicated in Fig. 2.

The core samples were prepared and counted in the same way as the modern samples (the counts are published with the modern abundances in the electronic supplement). SST reconstructions based on the radiolarian data were attempted for the LGM samples using four techniques available in Juggins' (2003) C2 software: weighted averaging regression and calibration (WA) (Birks et al., 1990), WA partial least squares (WA-PLS) (ter Braak and Juggins, 1993), Maximum Likelihood Method (MLM) (ter Braak et al., 1993), and the Modern Analog Technique (MAT) (Hutson, 1977). The SST estimates appear in Table 3 and the performance details in Table 4. The WA classical method results are not reported here because of their similarity to WA with inverse deshrinking (WA with classical deshrinking is used if the sample being reconstructed lies near the centre of the range of the training set and WA with inverse deshrinking if it lies close to either extreme). Similarly, the MAT weighted average are not reported because they are virtually identical to the MAT results. Two other methods, QMFA (Imbrie and Kipp, 1971) and SIMMAX (Pflaumann et al., 1996) (not available in C2) were examined but were not pursued for the same reasons as given in Barrows and Juggins (2005), and because their performance statistics were poor relative to other methods.

The SSTs for the six fossil samples were reconstructed using annual, austral summer, and austral winter WOA01 data as the environmental training sets and the eastern sector and the combined eastern and southern sectors radiolarian data as species training sets. Similarity Indices (Hammer et al., 2001; Hammer and Harper, 2006) indicated that there was little similarity between the fossil samples and any of the southern sector sites. As a result, no attempt was made to reconstruct LGM conditions using the southern sector data alone.

The reconstructions were compared with the Barrows and Juggins' (2005) estimates on the basis that Barrows and Juggins' T_{mean}, T_{max}, and T_{min} correspond to our study's SST estimates derived from WOA01 annual, austral summer, and austral winter data respectively. WA-PLS, whether applied to the combined data or the eastern sector data alone, generally gives values closer to Barrows and Juggins' (2005) estimates (which were derived using a consensus of MAT, the revised analog method, and artificial neural network results) than WA, MLM, or MAT (Table 3). Two-thirds of the estimates

Table 4
Performance statistics for the regression and calibration techniques investigated when reconstructing SSTs

Radiolarian data		Method									
		WA inverse		WA-PLS		MAT		MLM		QMFA	
		RMSEP	r^2	RMSEP	r^2	RMSEP	r^2	RMSEP	r^2	RMSEP	r^2
Eastern sector	Annual	1.24	0.89	1.07	0.94	1.33	0.79	1.53	0.84	1.35	0.83
	Summer	1.25	0.88	1.08	0.94	1.37	0.79	1.56	0.86	1.36	0.82
	Winter	1.16	0.88	1.03	0.94	1.27	0.77	1.25	0.94	1.29	0.82
Southern sector	Annual	2.10	0.86	2.07	0.93	2.35	0.85	1.87	0.92	2.59	0.81
	Summer	2.24	0.87	2.18	0.93	2.47	0.87	2.05	0.92	2.71	0.82
	Winter	1.99	0.87	1.97	0.93	2.24	0.84	1.80	0.92	2.40	0.82
Combined eastern and southern sectors	Annual	2.56	0.92	1.79	0.98	1.77	0.97	1.69	0.97	2.62	0.92
	Summer	2.63	0.92	1.82	0.98	1.78	0.97	1.74	0.97	2.61	0.92
	Winter	2.42	0.93	1.70	0.98	1.67	0.97	1.53	0.98	2.50	0.92

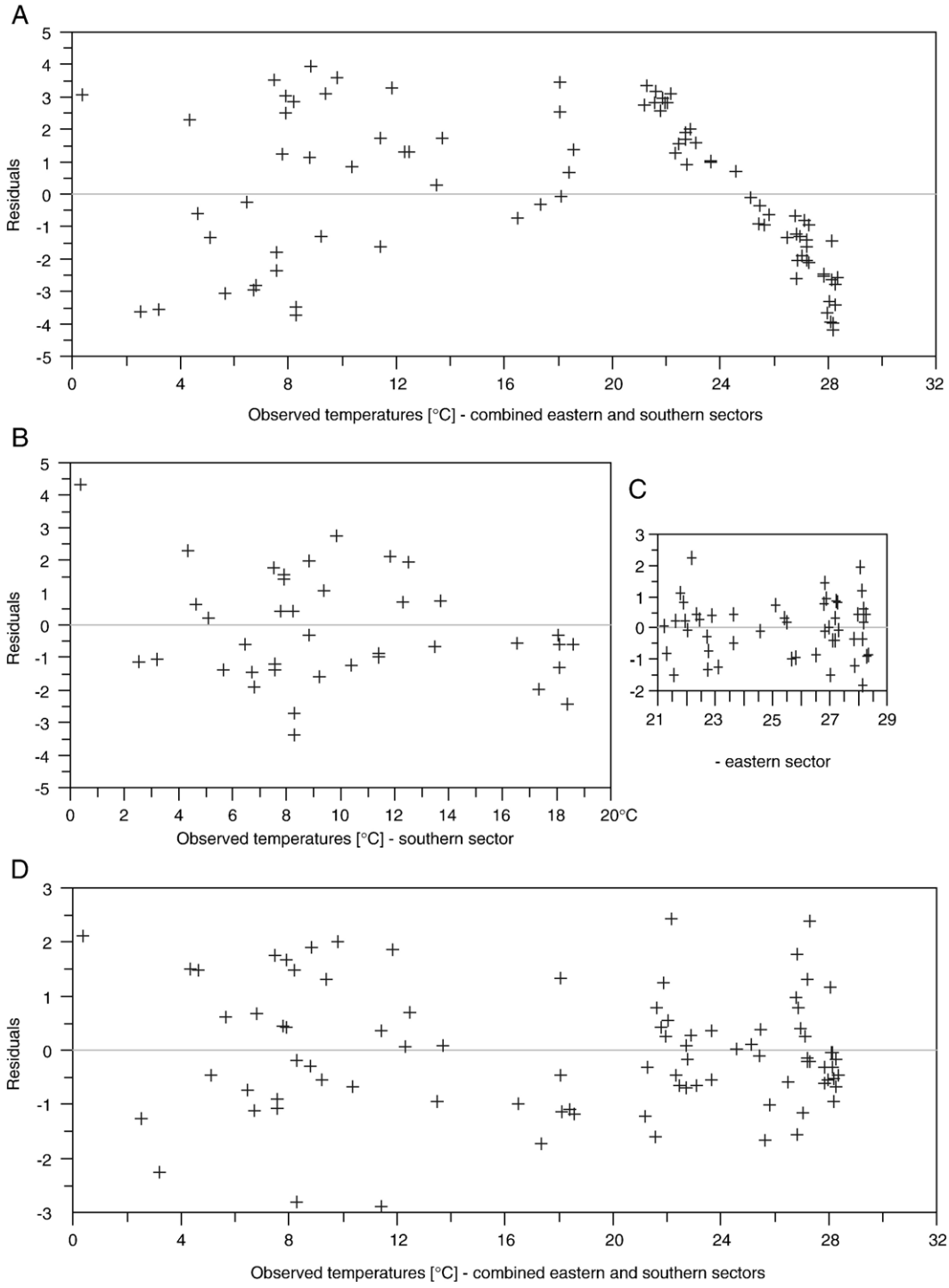

Fig. 7. The residuals obtained from regressions plotted against the observed SSTs. A: WA regression using the combined eastern and southern radiolarian data; B: WA regression using the southern data alone; C: WA regression using the eastern data alone; D: WAPLS regression using the combined eastern and southern radiolarian data. Note the linear relationship between the residuals and the observed values above 20 °C in A which does not appear in C or D.

Table 5
The WOA01 interpolations and WA-PLS predictions of modern SST, NTA, salinity, phosphate, dissolved oxygen, density, and nitrate at the sea-surface derived from the combined eastern and southern data for the LGM sample cores

Environmental variable	Core	Surface sediment estimates ± 1 standard error		LGM estimates ± 1 standard error		
		Interpolated from WOA01	WA-PLS predictions	Depth [cm]	RMSEP/r^2	Reconstruction
SST [°C]	Fr10/95-GC11	27.0±0.2	25.9±1.7	27.0	1.79/0.98	24.5±0.7
	Fr10/95-GC14	25.8±0.4	24.8±1.2	45.0		23.4±0.5
	Fr10/95-GC17	25.4±0.1	25.3±0.4	127.0		24.3±0.5
	Fr10/95-GC20	23.7±0.1	23.1±0.5	54.0		20.8±0.7
	Fr02/96-GC10	22.9±0.3	23.0±0.8	20.0		21.3±0.7
				22.0		22.3±0.6
NTA-alkalinity [μmol/l]	Fr10-95-GC11	2291±4	2292±1.0	27.0	5.94/0.93	2296±0.7
	Fr10-95-GC14	2291±4	2291±1.1	45.0		2290±0.5
	Fr10-95-GC17	2291±4	2293±0.7	127.0		2294±0.5
	Fr10-95-GC20	2291±4	2291±0.8	54.0		2289±0.6
	Fr02-96-GC10	2291±4	2291±1.0	20.0		2298±0.8
				22.0		2295±0.6
Salinity [PSU]	Fr10/95-GC11	34.76±0.07	34.92±0.31	27.0	0.21/0.93	34.80±0.08
	Fr10/95-GC14	34.96±0.06	35.14±0.05	45.0		35.42±0.07
	Fr10/95-GC17	35.09±0.03	35.93±0.04	127.0		35.03±0.08
	Fr10/95-GC20	35.36±0.03	36.43±0.04	54.0		35.95±0.10
	Fr02/96-GC10	35.41±0.07	35.32±0.07	20.0		35.02±0.07
				22.0		35.14±0.08
Phosphate concentration [μmol/l]	Fr10-95-GC11	0.13±(n/a)	0.14±0.02	27.0	0.12/0.96	0.30±0.04
	Fr10-95-GC14	0.15±0.01	0.14±0.02	45.0		0.12±0.02
	Fr10-95-GC17	0.18±0.02	0.16±0.02	127.0		0.23±0.03
	Fr10-95-GC20	0.14±0.01	0.11±0.02	54.0		0.09±0.04
	Fr02-96-GC10	0.13±0.03	0.13±0.02	20.0		0.34±0.03
				22.0		0.26±0.03
Dissolved oxygen [μmol/l]	Fr10-95-GC11	4.61±0.04	4.67±0.03	27.0	0.23/0.98	4.87±0.08
	Fr10-95-GC14	4.67±0.11	4.76±0.03	45.0		4.89±0.05
	Fr10-95-GC17	4.67±0.07	4.72±0.03	127.0		4.86±0.05
	Fr10-95-GC20	4.88±0.04	4.90±0.03	54.0		5.08±0.07
	Fr02-96-GC10	4.89±0.09	4.88±0.03	20.0		5.16±0.08
				22.0		5.03±0.07
Density [kg/m^3]	Fr10-95-GC11	1022.5±0.1	1023.00±0.1	27.0	0.41/0.98	1023.1±0.2
	Fr10-95-GC14	1023.1±0.2	1023.41±0.1	45.0		1023.8±0.2
	Fr10-95-GC17	1023.3±0.1	1023.18±0.1	127.0		1023.4±0.2
	Fr10-95-GC20	1024.0±0.1	1024.20±0.1	54.0		1024.9±0.2
	Fr02-96-GC10	1024.3±0.1	1024.10±0.1	20.0		1024.2±0.2
				22.0		1024.2±0.2
Nitrate concentration [μmol/l]	Fr10-95-GC11	0.39±(n/a)	0.94±0.28	27.0	2.27/0.96	2.52±0.48
	Fr10-95-GC14	0.34±(n/a)	0.27±0.28	45.0		−0.56±0.37
	Fr10-95-GC17	0.19±(n/a)	0.75±0.27	127.0		1.42±0.46
	Fr10-95-GC20	0.36±(n/a)	0.87±0.30	54.0		−1.28±0.62
	Fr02-96-GC10	0.43±(n/a)	0.52±0.34	20.0		2.72±0.49
				22.0		1.88±0.46

The LGM reconstructions of the same variables with the performance data (RMSEP and r^2). The negative values for nitrate are explained in the text.

from WA-PLS applied to the combined data are within 1 °C, and all are within two standard errors, of estimates based on planktonic foraminifera (Barrows and Juggins, 2005).

The WA-PLS Root Mean Squared Errors of Prediction (RMSEPs) are less than 2 °C in most cases and lower than those for other methods except MLM and the WA-PLS r^2 values (the squared correlations between inferred and observed values) are higher than for the other methods (Table 4). In addition, the residuals (the differences between the observed and the predicted SST estimates) generated by applying any of the reconstruction techniques except WA-PLS to the combined radiolarian data are not normally distributed and the values for the eastern sector decrease approximately linearly with increasing temperature (Fig. 7). The WA-PLS residuals derived from the combined data are normally distributed (Fig. 7D), as are those derived from the eastern and southern sector data

when processed separately, regardless of the method used (Fig. 7B and C).

Palaeo-reconstructions of alkalinity, salinity, dissolved oxygen, density, and nitrate and phosphate concentrations at the sea-surface were generated for the six fossil samples using WA-PLS: the results are presented in Table 5.

5. Discussion

5.1. Radiolarian biogeography

Eleven distinct radiolarian assemblages have been identified in the study area and each is associated with a particular geographic area and with a specific combination of environmental parameters. Thus, each assemblage defines a biogeographic province. The identification of these provinces confirms and refines the work of previous researchers, particularly Johnson and Nigrini's (1982), in so far as their different analytic methods allow comparison. Comparison with Johnson and Nigrini's work is difficult because these authors restricted themselves to the presence or absence of 74 taxa: our study analysed the abundance counts of all except the rarest taxa present, namely 216 taxa. Thus, for example, Johnson and Nigrini (1982) did not include *Tetrapyle octacantha* in their assemblages because it is ubiquitous, but it is a strong factor in our study with over 20% occurrence in assemblages A–F against less than 4% in assemblages H–L (Fig. 8). Another obstacle arises because Johnson and Nigrini (1982) appear to have used much larger sample sizes than we did. Thus, they were able to identify a recurrent group consisting of three species, *Pterocanium praetextum eucolpum*, *Theocorythium trachelium dianae*, and *Trigonastrum* sp., for temperate latitudes, whereas only one specimen of *P. praetextum eucolpum* was observed during our study and none of the other two species.

The assemblages G–L broadly map the five water masses bounded by the Northern and Southern Subtropical, the Subantarctic, and the Polar Fronts (Fig. 1). Exact correspondence between the assemblages and the water masses can be expected to be disrupted by seasonal and other variations in the location of the fronts and by the drift of the radiolarian tests as they fall through the water column. Using Tomczak and Godfrey's (1994) estimate of the Antarctic Circumpolar Current's speed range (0.05–0.15 m s^{-1}) and Takahashi's (1983) average sinking speeds (Nassellaria 30 m d^{-1}; Spumellaria 80 m d^{-1}) gives a minimum drift of 130 km and a maximum of 1000 km or about 2.0–20.0° of longitude at 45° S. Because, from surface to seabed, the drift is approximately parallel to the fronts bounding the assemblages (Tomczak and Godfrey, 1994), it will cause a relatively small eastward (and negligible northerly or southerly) displacement of the sub-fossils assemblages from their in vivo habitats. Geographically, assemblages G–K also correspond very closely with Johnson and Nigrini's (1982) Temperate, Transitional, Subpolar, and Polar Front Assemblages (VI–IX) respectively and, as far as it can be tested, the compositions of the assemblages are also very similar. The Johnson and Nigrini material does not extend sufficiently far south to distinguish this study's assemblage L.

Only a limited number of Johnson and Nigrini's (1982) 74 sample sites are close to the Western Australian coast: specifically, two sites lie in this study's environmental province A, two in C with two more close, three close to province F, and none in B, D, or E. Despite this and the differences between presence–absence and abundance data, it is possible to confirm some of their findings and develop others. Johnson and Nigrini (1982) identify three assemblages (III–V) in our eastern sector. Their Tropical assemblage (III) covers this study's assemblage A and B and is compositionally similar. Limited data would have made it difficult for Johnson and Nigrini (1982) to find a distinction between assemblages A and B as they had no sample site covering the assemblage B. Their South Equatorial assemblage (IV) geographically includes most of our assemblage C and the whole of D, and their Central Assemblage (V) corresponds with our assemblages E and F. Actually, using their recurrent group criteria, the South Equatorial (IV) assemblage is seen to extend as far south as 27° S, encompassing the whole of assemblage E and, perhaps, part of F. This is consistent with assemblage IV being associated with the Equatorial Gyral Current which flows eastwards through the latitude of assemblage IV, then splits, part turning south along the coast of Western Australia. In other words, instead of strictly following lines of latitude as Johnson and Nigrini (1982) show them, the assemblages are deflected southwards by the currents as the Western Australian coast is approached.

Further confirmation of the validity of our study's radiolarian provinces comes from Martínez et al. (1998) who investigated the same eastern sector core tops as used here. These latter authors report five planktonic foraminiferal provinces which correspond exactly with the location of this study's radiolarian assemblages except in that their Western Pacific Warm Pool province II covers three radiolarian assemblages, B, C, and D.

5.2. The association with oceanic parameters

The statistical analyses presented here reduces the number of WOA01 (2001) environmental variables

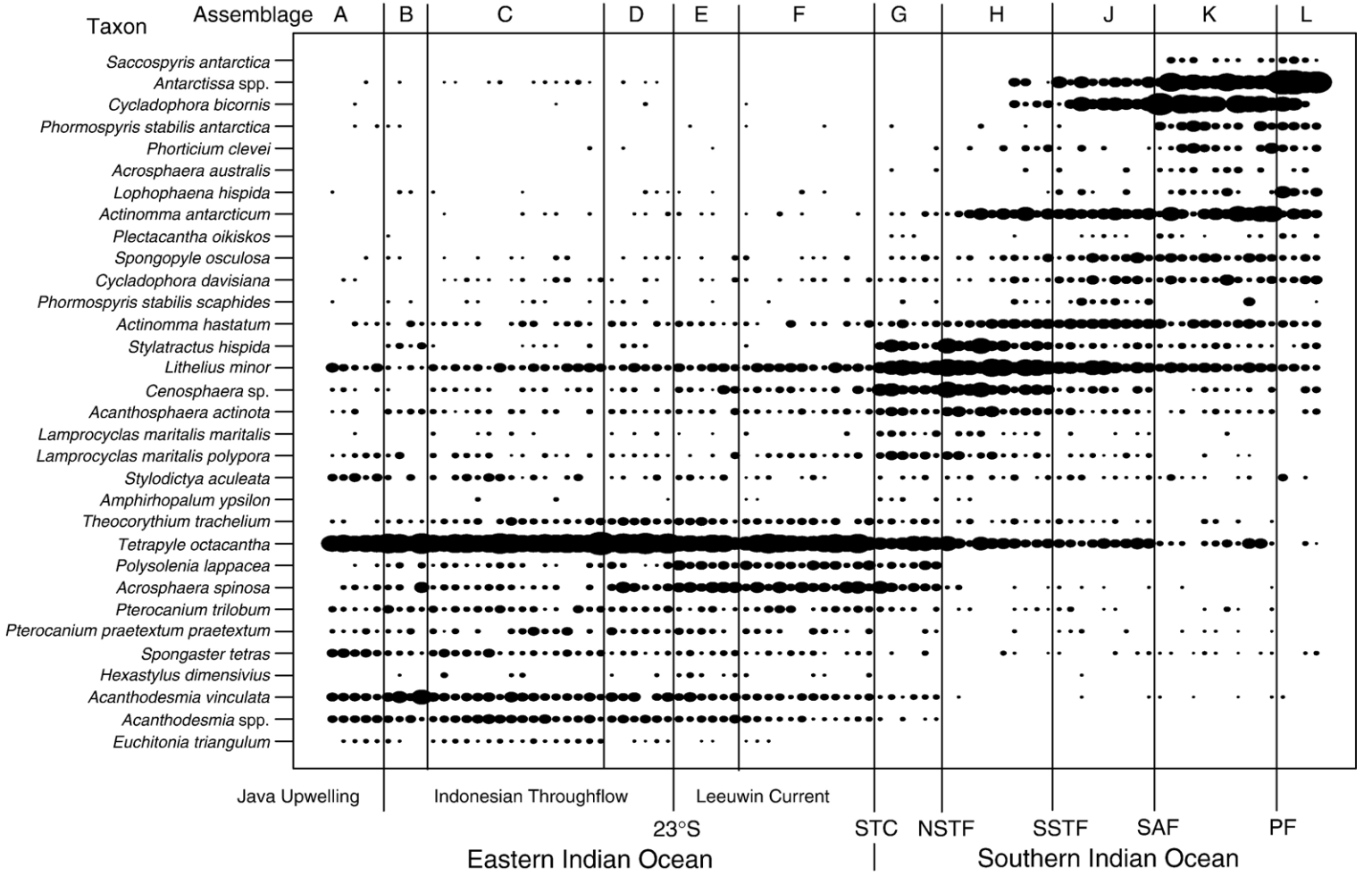

Fig. 8. An abundance plot of the indicator species (Table 2) by assemblage cluster (which approximately equates to latitude). The size of the "inkspots" is proportional to the percentage of the corresponding taxa in the site sample. Assemblage labels as Table 1 and abbreviations as Fig. 1.

which might explain the observed radiolarian distributions to five parameters and their derivatives. These five parameters are temperature, salinity, dissolved oxygen, and the nutrients, nitrate and phosphate; the derivates are NTA, density, and P*. Statistical argument says that, for the results not to indicate a causal relationship between these environmental parameters and the radiolarian assemblages, is so improbable as to be incredible. However, this relationship cannot be taken for granted, especially if the conclusion drawn is that Radiolaria respond to all five factors when it is equally possible that response is to one or two environmental factors, the other three or four coincidentally varying in parallel with the explanatory parameters.

Radiolarian response to temperature is well established and confirmed by comparison with results from other proxies (Vénec-Peyré et al., 1995; Pisias et al., 1997; Abelmann et al., 1999; Dolven et al., 2002). A connection with salinity is less certain but Gupta (2003) reports the existence of salinity-sensitive Radiolaria in the central Indian Ocean, Itaki et al. (2004) report the same for the Japan Sea, and Granlund (1986) found an association between salinity and the morphology of *Antarctissa* in the southern Indian Ocean. The relationship between radiolarian assemblages and nutrients such as nitrate and phosphate may be an indirect effect with the assemblages reflecting productivity which, in its turn, reflects nutrient levels (Caulet et al., 1992; Kling and Boltovskoy, 1995; Jacot Des Combes et al., 1999; De Wever et al., 2001). Dissolved oxygen as an explanatory variable is ecologically credible but the effects of variations in its concentrations [as opposed to the absence of Radiolaria under anoxic conditions (Itaki et al., 2004, 2007)] do not seem to have been reported previously: establishment of a causal relationship, therefore, will require a body of confirmatory evidence. Similarly, there is apparently no published ecological evidence for alkalinity as a determinant of radiolarian distribution. The response to density is slightly weaker than to the other parameters, perhaps indicating that temperature and salinity, which are determining factors for density, are the actual explanatory variables.

5.3. A window into the past: the LGM

Reconstructions of five LGM parameters (temperature, salinity, dissolved oxygen, and the concentrations of nitrate and phosphate) are justified because of the large percentage (>25%) of the radiolarian data variance explained by these environmental parameters. Estimates of the five LGM parameters at the surface of the eastern Indian Ocean have been obtained using WA-PLS regression and calibration (Table 5) and it would be possible to reconstruct the same parameters at all depths in the mixed layer for which modern data is available. The credibility of the results is particularly enhanced by the closeness of the LGM SST estimates to those of Barrows and Juggins (2005). Further, the span of our study's data means that reconstructions of the same parameters would be possible, given suitable fossil samples, for a substantial part of the southern Indian Ocean.

The estimation of the salinity-normalised total alkalinity (NTA) at the sea-surface is also justifiable as NTA explains in excess of 25% of the radiolarian abundance variance (Fig. 6 and the electronic supplement). Annual NTA has been estimated using Millero et al.'s (1998) empirical relationship (Table 5) and the modern values predicted using WA-PLS regression compared with those derived from the relationship (Fig. 9). The WA-PLS predictions fitted the Millero et al. (1998) values closely, emphasising the validity of the predictions. The reconstructed values for two of the three LGM samples south of 20° S and within the Leeuwin Current (Fr10/95-GC14 and -GC20) are slightly lower than modern values. The three samples from outside the LC (Fr10/95-GC11 and the two samples from Fr02/96-GC10) are noticeably higher than modern values. Fr10/95-GC17, a site which lies close to Western Australian coast, yields a value lying between these extremes.

South of 20° S and within the LC, salinity has fallen sharply since the LGM, and phosphate increased marginally (Table 5 and Fig. 10). By contrast, further from the Western Australian coast, salinity increased marginally and phosphate decreased by a factor of two to three. Fr10/95-GC17 shows changes between the extremes. The differences between our LGM reconstructions and modern values for NTA, salinity, and phosphate, all suggest that, between the LGM and the present, there has been a major change in ocean circulation south of 20° S. Most probably, during the LGM, the Leeuwin Current was inoperative along the Western Australian coast south of 20° S. The apparently ambiguous results for Fr10/95-GC17 are explicable by the core site's location much closer to the coast than the other four.

The fact that WA-PLS is, on the basis of performance criteria, apparently the best of the four methods used in this study to estimate LGM SSTs is not surprising because the method was designed to reduce the effects of the noise due to other environmental gradients (ter Braak and Juggins, 1993; ter Braak et al., 1993). As can been seen from Table 5, WA-PLS predictions for the modern values of environmental variables (with the exception of nitrate concentrations) are close to the WOA01 estimates. The estimates of nitrate concentrations in the LGM

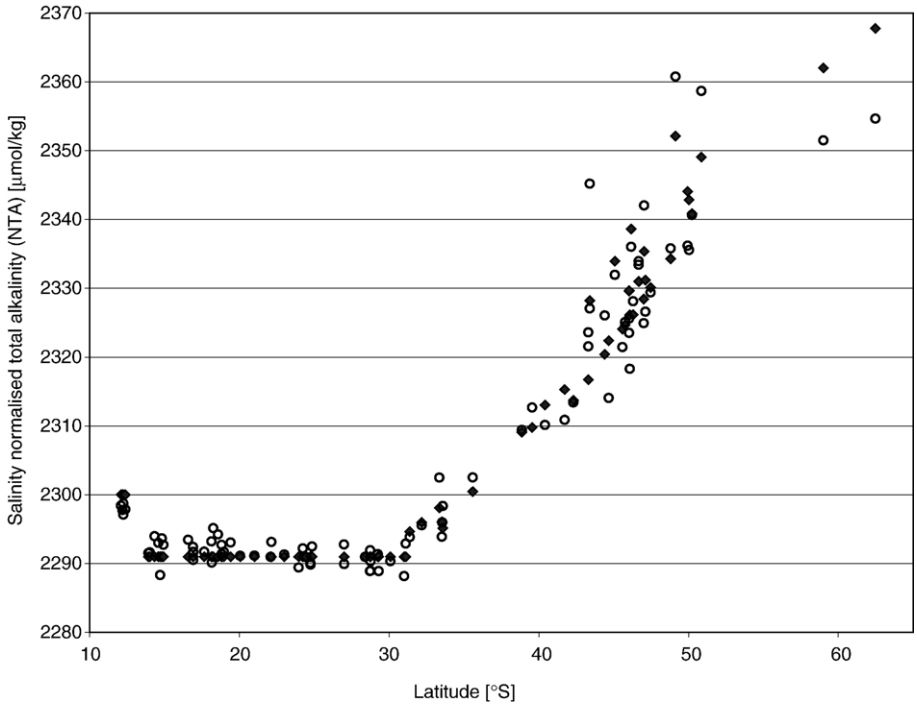

Fig. 9. Salinity-normalised total alkalinity (NTA): values derived from SSTs (Millero et al., 1998) (filled diamond) and those predicted under WA-PLS regression (open circles).

samples are poor because standard errors are of the same order as the expected values due to the high concentrations in the southern sector and very low concentrations in the eastern.

There are three possible sources of statistical noise in the eastern sector of the Indian Ocean which do not affect the southern sector we studied, any or all of which may explain the failure of any technique other than WA-PLS to provide credible reconstructions of past oceanographic conditions. Firstly, as ter Braak and Juggins (1993) indicate, WA-PLS is designed to use the structure of explanatory variables in addition to the one of interest, which other methods are not. There is the sharp reversal in the salinity gradient between approximately 30° S and 33° S, where the southward flowing Leeuwin Current meets the WAC, whereas the other explanatory variables have gradients reasonably close to linear over the two sectors. This is reflected in the fact that, for all the regression and calibration methods investigated except WA-PLS, the eastern Indian Ocean residuals vary directly with salinity and are not normally distributed about zero.

Secondly, due to the action of currents, microfossil tests are not deposited vertically below the habitat of the living organism. There will, therefore, always be some decoupling between the observed assemblages and the oceanographic parameters at the sites where the cores were taken. In the southern Indian Ocean, this dislocation is limited to a relatively small eastward drift of the dead plankton. In the eastern Indian Ocean, currents are very complex and it is possible that the decoupling is much more extreme.

Finally, in trying to explain the difference between foraminiferal- and radiolarian-based SST estimates for two cores from the southern Indian Ocean, Howard and Prell (1984) suggested the cause may be that planktonic foraminifera respond to surface oceanographic conditions whereas Radiolaria respond to the conditions of deeper waters. If conditions at the surface and in deeper waters were not precisely coupled, radiolarian responses would not necessarily reflect changes at the sea-surface. This hypothesis may also apply to our study because, for the most part, the highest CA correlations and the best CCA explanations of variance are obtained with environmental variables at a depth of 200 m when the southern or the combined radiolarian data is analysed. As a development on the Howard and Prell hypothesis, our eastern sector data appears dominated by Radiolaria which live in the mixed layer and deeper-dwelling species in the southern sector. This is evidenced by the fact that the best eastern sector correlations are, unlike those of the southern sector,

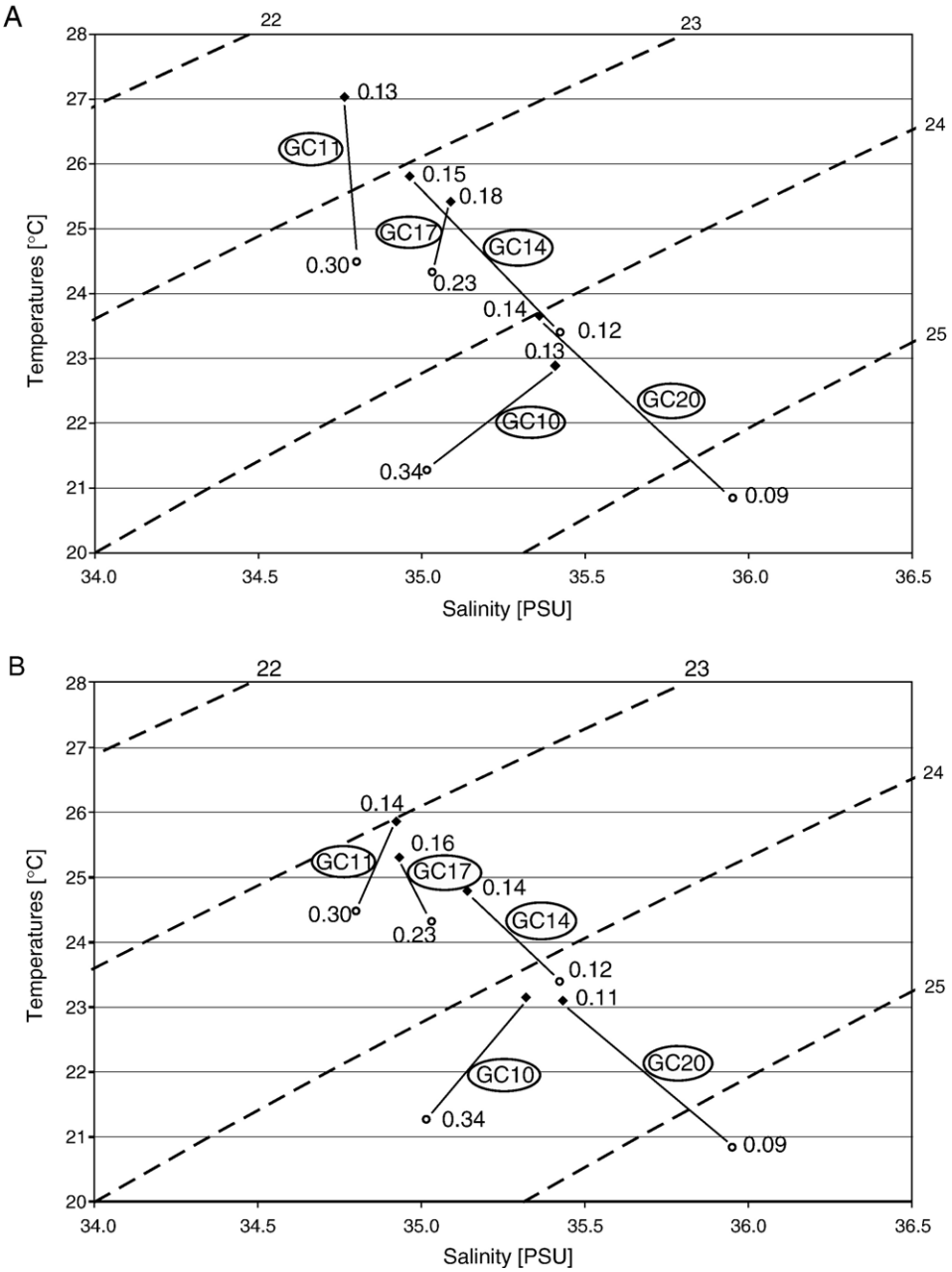

Fig. 10. SST estimates of the core top and LGM samples plotted against their salinities for five sites in the eastern Indian Ocean (see Table 1 and Fig. 2). Modern values (diamonds) are linked to their LGM reconstructions (circles) by solid lines with the core designators in ovals. Estimates of phosphate concentration [μmol/l] appear next to each point; the dashed lines are isopycnals. A: NOAA modern estimates; B: WA-PLS modern estimates. Estimates for Fr02/96-GC10 are omitted for clarity. Note the broad shifts over the isopycnals lines between the LGM and today.

with environmental variables at the surface or 50 m. In addition, the WADE Index (Lazarus et al., 2006), being the ratio of mixed layer species to intermediate water species, is 7.9 for the eastern sector against 0.4 for the southern. If, as seems probable, our eastern sector abundance counts more strongly reflect surface phenomena, and those from the southern sector, deeper water conditions, it is not surprising that most conventional regression and calibration techniques produce less than credible reconstructions. This hypothesis, which we prefer, would also explain why foraminiferal studies could use statistical techniques we were forced to reject:

the foraminiferal tests investigated in any particular study come from a more limited section of the water column than radiolarians from the same samples.

The question arises as to why other researchers do not report this problem. Two previous researchers have generated transfer functions from radiolarian samples from the eastern and southern Indian Oceans. Dow (1978) drew her samples solely from the southern sector south of 40° S: the discontinuity at 31° S does not, therefore, affect her conclusions. Morley's (1989) samples were drawn from between 21.7° S and 59.0° S and should be affected. However, only one of his samples lies in this study's eastern sector and none in Johnson and Nigrini's (1982) Central Assemblage. Morley (1989), thus, had insufficient data to reveal the discontinuity between this study's eastern and southern sectors and evidently found no similar problem in the western Indian Ocean where Johnson and Nigrini's (1982) South Equatorial Current (IV) and Temperate Assemblages (VI) are contiguous.

5.4. Productivity indicators

The WADE index, which Lazarus et al. (2006) have determined to be a good indicator of productivity, changes by a factor of eighteen at the boundary of the eastern and southern sectors (31° S) (Table 1). This indicates the eastern sector has much higher productivity than the southern. The phenomenon may be due to the effects of nutrients carried by the Java Upwelling in the eastern sector's north, an upwelling close to the coast at about 22° S (Goes et al., 2004), and the WAC, LUC, and coastal currents between 31° S and 22° S. The assemblages with the highest WADE values are those between 20° S and 25° S where Goes et al. (2004) reported high nitrate concentrations. Both the WADE index and the URI have a wide variance when calculated on a sample-site basis, suggesting that individual measurements have limited utility. Overall, the URI shows no strong features, probably because the radiolarian sample sizes are too small.

5.5. Further observations on the distribution of taxa

The order Collodaria is poorly represented in assemblage A, the assemblage close to the Java Upwelling: it comprises only 3% of the total specimens and no species dominates. Below 33° S, Collodaria are also very sparse, making up only 1.5% of the population, but the order constitutes approximately 13% of the total radiolarian population in assemblages B–G, i.e. 10° and 33° S, with four species, *Acrosphaera spinosa*, *Collosphaera huxleyi*, *Polysolenia lappacea*, and *Sphaerozoum punctatum*, making up three quarters of the specimens (the distributions of *A. spinosa* and *P. lappacea* are shown in Fig. 8). These four species probably derive their nutriment from photosynthetic algae (Haeckel, 1887), so their presence in low latitudes and absence from higher ones is to be expected. Fig. 8 illustrates the distribution of the indicator species (Dufrêne and Legendre, 1997) and brings out the very large species changes across the southern sector with *Cenosphaera*sp., *Stylosphaera hispida*, and *Lithelius minor* dominating around 40° S and *Actinomma antarcticum*, *Cycladophora bicornis*, and *Antarctissa* spp. at 50° and further south. Much less variation is apparent in the eastern sector.

6. Conclusions

The radiolarian species distribution in the southern Indian Ocean is principally determined by a package of environmental factors in the mixed layer: water temperature, alkalinity, and salinity, dissolved oxygen, and the concentrations of two nutrients, nitrate and phosphate. In this sector, these factors change together in a regular fashion, creating a strong ecological gradient and a clear change in the radiolarian species distributions across the region. In the eastern Indian Ocean, the radiolarian response to temperature, salinity, and dissolved oxygen is evident but is weaker than in the southern sector. The concentrations of nitrate and phosphate vary barely enough for a radiolarian response to be detected and NTA is virtually unchanging. However, when the eastern and southern sector datasets are combined, the correlation between radiolarian distribution and all the environmental factors (with the exception of salinity) is strongly enhanced.

Because, effectively, the explanatory variables behave as one, it is possible to produce reliable palaeoenvironmental reconstructions of all six as well as density because it is a function of temperature and salinity. Thus, radiolarian abundance is the first proxy to have been established for alkalinity, salinity, density, dissolved oxygen, and the concentrations of nitrate and phosphate, this not having been achieved thus far using other microscopic organisms. Using this proxy to reconstruct ocean parameters, we can say the Leeuwin Current was probably not flowing south of 20° S during the LGM.

The predominance of mixed-layer dwelling Radiolaria in the eastern sector and of deeper-water taxa in the southern sector, the complexity of water movement, the abrupt reversal of the salinity gradient at the southernmost limit of the Leeuwin Current (33° S), or a combination of these factors, prevents the application of the most commonly used techniques to obtain palaeoenvironmental reconstructions from our radiolarian data. Only WA-

PLS provides results comparable with other estimates. This finding represents a major step in the statistical analysis of radiolarian populations whose variety of habitat and trophic type demands more sophisticated techniques than other microfossils. The use of WA-PLS with our data resolves the discrepancy between radiolarian-based reconstruction of palaeo-SSTs and those obtained by other methods. At the same time, the commonly-used statistical techniques may be successfully applied if the study area is partitioned, similarity indices being employed to determine which partition is appropriate to a particular reconstruction.

The discovery of more radiolarian provinces than previously known in these sectors of the Indian Ocean, and the better definition of some of those previous recognised, has the potential to allow the mapping of past oceanic conditions in the southern and eastern Indian Ocean such as the movements of currents and fronts.

Acknowledgements

We are grateful to Drs. E. Michel and J.L. Turon for access to the RV *Marion Dufresne* samples; also to Dr. J. Wood for statistical advice, to Dr. S. Juggins both for statistical advice and R scripts, to Dr I.M. Belkin for ocean front data, to Dr A. Hogg for oceanographic information, and to Dr M. Ellwood for discussions on geochemistry. We would also like to thank Dr. G. Cortese, Dr. Ø. Hammer, and an anonymous referee for their thorough reviews of an earlier version of this paper and their very pertinent comments. Further, we would like to thank Dr E. Thomas for the great help she has given in the paper's preparation.

The RV *Franklin* samples were obtained through grants to PDD from the Australian National Facility, the Australian Research Council, and the Australian National University Small Research Grant Scheme awarded several years ago. JR is funded with an Australian Postgraduate Award.

Appendix A. Supplementary data

Supplementary data associated with this article can be found, in the online version, at doi:10.1016/j.marmicro.2007.07.001.

References

Abelmann, A., Brathauer, U., Gersonde, R., Sieger, R., Zielinski, U., 1999. Radiolarian-based transfer function for the estimation of sea surface temperature in the Southern Ocean (Atlantic Sector). Paleoceanography 14 (3), 410–421.

Bareille, G., Grousset, F., Labracherie, M., 1994. Origin of detrital fluxes in the southeast Indian Ocean during the last climatic cycles. Paleoceanography 9 (6), 799–819.

Bareille, G., Labracherie, M., Bertrand, P., Labeyrie, L., Lavaux, G., Dignan, M., 1998. Glacial–interglacial changes in the accumulation rates of major biogenic components in Southern Indian Ocean sediments. Journal of Marine Systems 17, 527–539.

Barrows, T., Juggins, S., 2005. Sea-surface temperatures around the Australian margin and Indian Ocean during the Last Glacial Maximum. Quaternary Science Reviews 24, 1017–1047.

Belkin, I., Gordon, A., 1996. Southern Ocean fronts from the Greenwich meridian to Tasmania. Journal of Geophysical Research 101 (C2), 3675–3696.

Birks, H., 1994. The importance of pollen and diatom taxonomic precision in quantitative palaeoenvironmental reconstructions. Review of Palaeobotany and Palynology 83, 107–117.

Birks, H., Line, J., Juggins, S., Stevenson, A., Ter Braak, C., 1990. Diatoms and pH reconstruction. Philosophical Transactions of the Royal Society of London. Series B, Biological Sciences 327 (1240), 263–278.

Boltovskoy, D., 1998. Classification and distribution of South Atlantic Recent Polycystine Radiolaria. Palaeontologia Electronica 1 (2), 1–116.

Breiman, L., Friedman, J., Olshen, R., Stone, J., 1984. Classification and Regression Trees. Wadsworth, Belmont, Ca.

Caulet, J.-P., Vénec-Peyré, M.-T., Vergnaud Grazzaini, C., Nigrini, C., 1992. Variation of the South Somalian upwelling during the last 160 ka; radiolarian and foraminifera records in core MD 85674. In: Summerhayes, C., Prell, W., Emeis, K. (Eds.), Upwelling Systems: Evolution Since the Early Miocene. Geological Society of London, London, pp. 379–389.

Cresswell, G., 1991. The Leeuwin Current — observations and recent models. Journal of the Royal Society of Western Australia 74, 1–14.

Cresswell, G., Golding, T., 1980. Observations of a south-flowing current in the southeastern Indian Ocean. Deep-Sea Research 27A, 449–466.

De'ath, G., 2002. Multivariate regression trees: a new technique for modeling species–environment relationships. Ecology 83 (4), 1105–1117.

De Wever, P., Dumitrica, P., Caulet, J.-P., Nigrini, C., Caridroit, M., 2001. Radiolarians in the Sedimentary Record. Gordon and Breach Science Publishers, Amsterdam.

Deutsch, C., Sarmiento, J., Sigman, D., Gruber, N., Dunne, J., 2007. Spatial coupling of nitrogen inputs and losses in the ocean. Nature 445, 163–167.

Dezileau, L., Bareille, G., Reyss, J., Lemoine, F., 2000. Evidence for strong sediment redistribution by bottom currents along the southeast Indian ridge. Deep-Sea Research I 47, 1899–1936.

Dezileau, L., Bareille, G., Reyss, J., 2002. Enrichissement en uranium authigène dans les sédiments glaciaires de l'océan Austral. C.R. Comptes rendus de l'Academie des Sciences – Geoscience 334, 1039–1046.

Dolven, J., 2004. Radiolaria.org. http://www.radiolaria.org2004.

Dolven, J., Cortese, G., Bjørklund, K., 2002. A high-resolution radiolarian-derived paleotemperature record for the late Pleistocene–Holocene in the Norwegian Sea. Paleoceanography 17 (4), 24.1–24.13.

Dow, R., 1978. Radiolarian distribution and the Late Pleistocene history of the southeastern Indian Ocean. Marine Micropaleontology 3, 203–227.

Dufrêne, M., Legendre, P., 1997. Species assemblages and indicator species: the need for a flexible asymmetical approach. Ecological Monographs 67 (3), 345–366.

Fagel, N., Dehairs, F., André, L., Bareille, G., Monnin, C., 2002. Ba distribution in the surface Southern Ocean sediments and export production estimates. Paleoceanography 17 (2-1011), 1.1–1.20.

Fatela, F., Taborda, R., 2002. Confidence limits of species proportions in microfossil assemblages. Marine Micropaleontology 45, 169–174.

Feng, M., Meyers, G., Pearce, A., Wijffels, S., 2003. Annual and interannual variations of the Leeuwin Current at 32°S. Journal of Geophysical Research 108 (C11), 19/1–19/21.

Fieux, M., Andrié, C., Delecluse, P., Ilahude, A., Kartavtseff, A., Mantisi, F., Molcard, R., Swallow, J., 1994. Measurements within the Pacific-Indian Oceans throughflow region. Deep-Sea Research I 41 (7), 1091–1130.

Gingele, F., De Deckker, P., Hillenbrand, C.-D., 2001. Clay mineral distribution in surface sediments between Indonesia and NW Australia — source and transport by ocean currents. Marine Geology 179, 135–146.

Goes, J., Gomes, H., Saino, T., Wong, C., Mordy, C., 2004. Exploiting MODIS data for estimating sea surface nitrate from space. Eos Transactions 85 (44), 449–464.

Granlund, A., 1986. Size and shape patterns in the Recent Radiolarian genus *Antarctissa* from a South Indian Ocean transect. Marine Micropaleontology 11, 243–250.

Gupta, S., 2003. Orbital frequencies in radiolarian assemblages of the central Indian Ocean: implications on the Indian summer monsoon. Palaeogeography, Palaeoclimatology, Palaeoecology 197, 97–112.

Haeckel, E., 1887. Report on the Radiolaria collected by H.M.S. Challenger. In: Thompson, C., Murray, J. (Eds.), Report on the Scientific Results of the Voyage of HMS Challenger During the Years 1873–76. Her Majesty's Stationery Office, London, pp. 1–1803.

Hammer, Ø., Harper, D., 2006. Paleontological Data Analysis. Blackwell Publishing, Oxford.

Hammer, Ø., Harper, D.A.T., P.D., R., 2001. PAST: paleontological statistics software package for education and data analysis. Palaeontologia Electronica 4 (1).

Hill, M., 1980. Decorana. In: Oksanen, J., Kindt, R., Legendre, P., O'Hara, B. (Eds.), Library: "vegan" (version 1.8-3 (29 September 2006). http://cran.ms.unimelb.edu.au/).

Howard, W., Prell, W., 1984. A comparison of radiolarian and foraminiferal paleoecology in the southern Indian Ocean: new evidence for the interhemispheric timing of climate change. Quaternary Research 21, 244–263.

Hutson, W., 1977. Transfer functions under no-analog conditions: experiments with Indian Ocean Planktonic Foraminifera. Quaternary Research 8, 355–367.

Imbrie, J., Kipp, N., 1971. A new micropaleontological method for quantitative paleoclimatology: application to a late Pleistocene Caribbean Core. In: Turekian, K. (Ed.), The Late Cenozoic Glacial Ages. Yale University Press, New Haven, pp. 71–181.

Itaki, T., Ikehara, K., Motoyama, I., Hasegawa, S., 2004. Abrupt ventilation changes in the Japan Sea over the last 30 ky: evidence from deep-dwelling radiolarians. Palaeogeography, Palaeoclimatology, Palaeoecology 208, 263–278.

Itaki, T., Komatsu, N., Motoyama, I., 2007. Orbital- and millennial-scale changes in radiolarian assemblages during the last 220 kyrs in the Japan Sea. Palaeogeography, Palaeoclimatology, Palaeoecology 247, 115–130.

Jacot Des Combes, H., Caulet, J.-P., Tribovillard, N., 1999. Pelagic productivity changes in the equatorial area of the northwest Indian Ocean during the last 400,000 years. Marine Geology 158, 27–55.

Johnson, D., Nigrini, C., 1980. Radiolarian biogeography in surface sediments of the western Indian Ocean. Marine Micropaleontology 5, 111–152.

Johnson, D., Nigrini, C., 1982. Radiolarian biogeography in surface sediments of the eastern Indian Ocean. Marine Micropaleontology 7, 237–281.

Jongman, R., ter Braak, C., van Tongeren, O., 1987. Data Analysis in Community and Landscape Ecology. PUDOC Wageningen, Den Haag.

Juggins, S., 2003. C^2: Software for ecological and palaeoecological data analysis and visualisation. http://www.campus.ncl.ac.uk/staff/Stephen.Juggins/software/c2home.htm2003.

Kling, S., Boltovskoy, D., 1995. Radiolarian vertical distribution patterns across the southern California Current. Deep-Sea Research I 42 (2), 191–231.

Labeyrie, L., Labracherie, M., Gorfti, N., Pichon, J., Vautravers, M., Arnold, M., Duplessy, J.-C., Paterne, M., Michel, E., Duprat, J., Caralp, M., Turon, J.-L., 1996. Hydrographic changes over the Southern Ocean (southeast Indian sector) over the last 230 kyr. Paleoceanography 11 (1), 57–76.

Lazarus, D., Bittniok, B., Diester-Haass, L., Meyers, P., Billups, E., 2006. Comparison of radiolarian and sedimentologic paleoproductivity proxies in the latest Miocene–Recent Benguela Upwelling System. Marine Micropaleontology 60, 269–294.

Legendre, P., Legendre, L., 1998. Numerical Ecology. Elsevier, Amsterdam.

Martínez, J., De Deckker, P., Barrows, T., 1999. Palaeoceanography of the last glacial maximum in the eastern Indian Ocean: planktonic foraminiferal evidence. Palaeogeography, Palaeoclimatology, Palaeoecology 147, 73–99.

Martínez, J., Taylor, L., De Deckker, P., Barrows, T., 1998. Planktonic foraminifera from the eastern Indian Ocean: distribution and ecology in relation to the Western Pacific Ocean Warm Pool (WPWP). Marine Micropaleontology 34, 121–151.

Meyers, G., Bailey, R., Worby, A., 1995. Geostrophic transport of Indonesian throughflow. Deep-Sea Research I 42 (7), 1163–1174.

Millero, F., Lee, K., Roche, M., 1998. Distribution of alkalinity in the surface waters of the major oceans. Marine Chemistry 60, 111–130.

Morley, J., 1989. Radiolarian-based transfer functions for estimating paleoceanographic conditions in the Southern Ocean. Marine Micropaleontology 13, 293–307.

Murgese, S., De Deckker, P., 2005. The distribution of deep-sea benthic foraminifera in core tops from the eastern Indian Ocean. Marine Micropaleontology 56, 25–49.

Murtagh, F., *hclust*. In library: "stats", version 2.4.1 http://www.r-project.org.

Nigrini, C., Caulet, J.-P., 1992. Late Neogene radiolarian assemblages characteristic of Indo-Pacific areas of upwelling. Micropaleontology 38 (2), 139–164.

Nigrini, C., Moore, T.C., 1979. A Guide to Modern Radiolaria (online). http://gdcmp1.ucsd.edu/geol_coll/radlit/nm79titl.html1979.

Nigrini, C., Caulet, J.-P., Sanfilippo, A., 2004. RadWorld. http://www.mnhn.fr/mnhn/geo/radworld/radworldsite/radsearch.html2004.

Pearce, A., 1991. Eastern boundary currents of the southern hemisphere. Journal of the Royal Society of Western Australia 74, 35–45.

Pearce, A., Cresswell, G., 1985. Ocean circulation off Western Australia and the Leeuwin Current. CSIRO Information Service 16 (3).

Pearce, A., Pattiaratchi, C., 1999. The Capes Current: a summer countercurrent flowing pass Cape Leeuwin and Cape Naturaliste, Western Australia. Continental Shelf Research 19, 401–420.

Pearce, A., Phillips, B., 1988. ENSO events, the Leeuwin Current, and larval recruitment of the western rock lobster. Journal of the International Council for the Exploration of the Sea 45, 13–21.

Petrushevskaya, M., 1967. Radiolaria in the plankton and Recent sediments from the Indian Ocean and Antarctic. In: Funnell, B.,

Riedel, W. (Eds.), The Micropalaeontology of the Oceans. Cambridge University Press, Cambridge, pp. 319–330.

Pflaumann, U., Duprat, J., Pujol, C., Labeyrie, L., 1996. SIMMAX: a modern analog technique to deduce Atlantic sea surface temperatures from planktonic foraminifera in deep-sea sediments. Paleoceanography 11 (1), 15–35.

Pichon, J., Bareille, G., Labracherie, M., Labeyrie, L., Baudrimont, A., Turon, J.-L., 1992. Quantification of biogenic silica distribution in Southern Ocean sediments. Quaternary Research 37 (3), 361–378.

Pisias, N., Roelofs, A., Weber, M., 1997. Radiolarian-based transfer functions for estimating mean surface ocean temperatures and seasonal range. Paleoceanography 12 (3), 365–379.

Quadfasel, D., Frische, A., Cresswell, G., 1996. The circulation in the source area of the South Equatorial Current in the eastern Indian Ocean. Journal of Geophysical Research 101 (C5), 12483–12488.

R Development Core Team, 2004. R: a language and environment for statistical computing. http://www.R-project.org2004.

Sarmiento, J., Gruber, N., Brzezinski, M., Dunne, J., 2004. High-latitude controls of thermocline nutrients and low-latitude biological productivity. Nature 427 (6969), 56–60.

Schlitzer, R., 2005. Ocean Data View. http://www.awi-bremerhaven.de/GEO/ODV2005.

Smith, R., Huyer, A., Godfrey, J., Church, J., 1991. The Leeuwin Current off Western Australia, 1986–1987. Journal of Physical Oceanography 21, 323–345.

Takahashi, K., 1983. Radiolaria: sinking population, standing stock, and production rate. Marine Micropaleontology 8, 171–181.

Takahashi, K., Okada, H., 2000. The paleoceanography for the last 30,000 years in the southeastern Indian Ocean by means of calcareous nannofossils. Marine Micropaleontology 40, 83–103.

Taylor, J., Pearce, A., 1999. Ningaloo Reef Currents: implication for coral spawn dispersal, zooplankton, and whale shark abundance. Journal of the Royal Society of Western Australia 82, 57–65.

ter Braak, C., Juggins, S., 1993. Weighted averaging partial least squares regression (WA-PLS): an improved method for reconstructing environmental variables from species assemblages. Hydrobiologia 269/270, 485–502.

ter Braak, C., Verdonschot, P., 1995. Canonical correspondence analysis and related multivariate methods in aquatic ecology. Aquatic Sciences 57 (3), 255–289.

ter Braak, C., Juggins, S., Birks, H., van der Voet, H., 1993. Weighted averaging partial least squares regression (WA-PLS): definition and comparison with other methods for species–environment calibration. In: Patil, G., Rao, C. (Eds.), Multivariate Environmental Statistics. North Holland Series in Statistics and Probability. Elsevier Science Publishers, Amsterdam, pp. 525–560.

Thompson, R., 1983. Observations of the Leeuwin Current off Western Australia. Journal of Physical Oceanography 14, 623–648.

Tomczak, M., Godfrey, J., 1994. Regional Oceanography: an Introduction. Pergamon, Oxford.

van de Paverd, P., 1995. Recent Polycystine Radiolaria from the Snellius-II Expedition. PhD Thesis, Free University, Amsterdam.

van der Kaars, S., De Deckker, P., 2003. Pollen distribution in marine surface sediments offshore Western Australia. Review of Palaeobotany and Palynology 124, 113–129.

Vénec-Peyré, M.-T., Caulet, J.-P., Grazzaini, C., 1995. Paleohydrographic changes in the Somali Basin (5°N upwelling and equatorial areas) during the last 160 kyr, based on correspondence analysis of foraminiferal and radiolarian assemblages. Paleoceanography 10 (3), 473–491.

Waelbroeck, C., Jouzel, J., Labeyrie, L., Lorius, C., Labracherie, M., Stiévenard, M., Barov, N., 1995. A comparison of the Vostok ice deuterium record and series from Southern Ocean core MD-88-770 over the last two glacial–interglacial cycles. Climate Dynamics 12, 113–123.

WOA01, 2001. World Ocean Atlas 2001. http://iridl.ldeo.columbia.edu/SOURCES/.NOAA/.NODC/.WOA01/.

Young, M., 2006. The distribution of organic-and calcareous-walled dinoflagellate cysts from the eastern Indian Ocean; a proxy for late Quaternary palaeo-oceanographic reconstructions. PhD Thesis, The Australian National University, Canberra.